



## Advances in ballistic penetrating impact simulations on thin structures using Smooth Particles Hydrodynamics: A state of the art

Shuangshuang Meng<sup>\*</sup>, Lorenzo Taddei, Nadhir Lebaal, Sébastien Roth

Laboratoire Interdisciplinaire Carnot de Bourgogne, Site UTBM, UMR 6303/Univ. Bourgogne Franche-Comté, UTBM, France

### ARTICLE INFO

**Keywords:**

High velocity impacts (HVI)  
Numerical simulations  
Smooth Particles Hydrodynamics  
Tensile instability

### ABSTRACT

Experimental tests, analytical modeling, empirical or semi-empirical fit, and numerical simulation, are different concepts and ways to study the complex mechanism of High-Velocity Impact (HVI). Mainly studied in the framework of the improvement of high strength material, the understanding of this physical process can help to optimize the structures submitted to HVI problems. Aerospace or aeronautic lightweight structures, body-armor or armor plates devices, and others should be investigated, taking into account the high-velocity impact loading in terms of ability to stop projectiles, in terms of mass optimization, in terms of reduction of injury appearance for the human body. At a numerical level, lots of approaches like finite element method, finite difference method, or particle methods have been developed, allowing modeling and predicting the behavior of a structure impacted by a projectile. Focusing on the last one, the Smooth Particles Hydrodynamics (SPH) method as the earliest meshless method has been widely developed in the last decades. The characteristic of particle modeling in the SPH method can avoid the typical weakness (mesh distortion) of the mesh-based method, and make it naturally suitable for the large deformation problems. It can be found in the literature that the SPH method has been widely applied to model the behavior of a mechanical structure, especially concentrating on thin-plate structures. This paper attempts to make a state of the art for recent advances concerning the perforation of thin plates in the context of ballistic impacts using SPH analysis.

### 1. Introduction

The mechanical behavior of structures under high-speed loadings is of main interest in vehicle engineering or military framework. Indeed, the material used in the design whatever is the context has to satisfy different requirements, especially criterion on protection ability, or lightweight. As an example of structures with these kinds of important requirements and optimal performances, body-armors can be cited with a primary need of human body protection and dissipation of energy when impacted by the projectiles, and also a need of lightweight and mobility for human ergonomic aspects [1,2]. This balance between different development requirements for the designs of such protection devices need a deep understanding of the behavior of the material under complex physical loadings such as ballistic impacts.

In the context of High-Velocity Impacts (HVI), and to conduct these investigations, several ways are possible, as described in the literature: [3,4]: analytical modeling, semi-empirical data fits, experimental tests and numerical modeling. Analytical modeling consists of developing mathematical equations based on physical parameters allowing

calculating physical parameters (mass of the projectile or drag coefficient), such as penetration or velocity-time history, velocity as a function of the displacement of the projectile in the target [5,6]. The complementarity of measurements and theory can define semi-empirical fits, which can also achieve interesting results and understanding of perforation impact [7,8]. The third way of investigation is widely explored in the literature, and consists of experimental setups, collecting data provided by sensors, imaging processing, video processing et al. [9, 10]. These experimental results are taken as a reference to compare and validate results obtained by analytical, semi-empirical, or numerical models. The latter way called numerical simulation is also widely developed in the literature since today's computational powers allow conducting high-performance calculations such as the finite element method (FEM) and finite difference method (FDM). Particularly, the FEM method as one of the typical grid-based methods is the main numerical tool for engineers because of its apparent advantages like (a) Lagrangian grid fixed on the moving material enables it easy to track and obtain the time history of any field variable; (b) irregular or complicated geometries can be modeled by using an irregular mesh; (c) it has been

\* Corresponding author.

E-mail address: [sébastien.roth@utbm.fr](mailto:sébastien.roth@utbm.fr) (S. Roth).

highly developed by academia and industry for a long time, and become a mature and comparatively commercialized approach. It also becomes a powerful predicting tool for the behavior of mechanical structures under HVI [11–13] in the past decades.

Although grid-based methods like FEM provide very interesting results, some numerical limitations still exist. Linked to the involved grids or meshes which often lead to large distortions of elements when solid structures are extremely deformed, the methods based on meshing technique are not very suitable for simulating hydrodynamic phenomena like explosion and HVI which typically include large deformations, moving material interfaces, deformable boundaries as well as fragmentations. The mesh distortion can cause significant errors in these analyses. To avoid it, other numerical concepts have been developed, based on particle discretization, also called meshfree or meshless methods like The Smoothed Particle Hydrodynamics method (SPH) [14, 15], Discrete Element Method (DEM) [16,17], Dissipative Particle Dynamics (DPD) [18], Material Point Method (MPM) [19] etc. Some reviews on the meshfree and particle methods and their differences can be found such as [20–22], but the SPH method as the earliest meshfree method and has been developed the most is the target of this review. It has been initially developed in the astrophysical field [14,15]. Since the nineties, some researchers have adapted this method to solid mechanics in the framework of HVI [23,24]. This method has been widely improved during the 20 last years and appears to be very promising for solid mechanics for the understanding of large deformed mechanics.

Compared to traditional grid-based numerical methods, some distinct benefits of the SPH method have been recognized during the various applications. (1) The particle modeling of Lagrangian nature in SPH can concern the time history of the material particles, which allows straightforward handling of very large deformations since the connectivity between particles are generated as part of the computation and can change with time. (2) The free surfaces, material interfaces, and moving boundaries can all be traced freely in the process of simulation, which is always challenging to many Eulerian methods. (3) The SPH method is a suitable alternative for non-continuum problems, typically examples involving bio- and nano-engineering at the micro and nano-scale, and astrophysics at astronomic scale, as well as the debris clouds phenomenon in HVIs. (4) SPH formulations are comparatively simple and easy to be developed or improved as 3D-codes by some algorithms or to be coupled with other numerical methods.

Because of these advantages, as well as the significant value of investigating the HVI process in engineering, this study attempts to review the Smooth Particles Hydrodynamics (SPH) method and its improvements applied to high-velocity impacts. Taking into account the very complicated and various mechanisms depending on the impact conditions, this review only highlights the response of thin structures under the high-velocity impact. Firstly, the definition of the thin target means the stress and deformation gradients throughout its thickness do not exist according to Ref. [25] which classified target by its thickness in impact problems. Also, penetration is a general description as to the sequence of impacts, which involves the perforation, embedment, ricochet, as well as the fragments and debris clouds with efficiently high velocity. Perforation means that the projectile passes through the target structure, embedment means that the projectile is stopped in the target that appears generally in enough thick structures. Ricochet means that the projectile is deflected from the target without perforating. The fragments and debris clouds are the most comment damage in the target structures caused by the projectile which passes out the target with very high impact velocity. In this study, particularized to the impacts of the thin structures, the mechanical problems like perforation, fragments, and debris clouds principally happen and thereby these properties would be emphasized in SPH simulations.

Therefore, the objective of this study is to review the simulations for high-velocity impacts by the SPH method in the past 30 years. Firstly, an introduction about standard SPH and its improvements, as well as its implementation in solids are represented, respectively, in section 2 and

3. Then, a state of the art about SPH simulating HVI problems is provided in section 4, followed by a discussion about existing limitations and improvements when SPH method modeling HVI problems in section 5. Finally, a conclusion shows some further research required in the development of the SPH simulating projectile-target system.

## 2. SPH fundamental theory

In SPH method, the entire computational domain is discretized into a number of particles that represent a certain volume of the material, and the particles hold material properties and interact with each other in a limited domain defined by a weight function or smoothing function  $W$ . Owing to its natural particle feature to track material movement flexibly, and the strong ability to incorporate complex physics into the SPH formulation, it has been extended to a large range of problems in both fluid and solid mechanics. This section mainly introduces the formulation of standard SPH by Refs. [14,15] and its developments during the last 30 years.

### 2.1. Standard SPH

Standard SPH also called conventional SPH initially developed in Refs. [14,15] is regarded as a typical meshfree numerical method based on particle modeling, which mainly consists of two processes, kernel approximation, and particle discretization. The first major process in SPH formulation is the kernel approximation, which approximates the field variables and their derivatives using the nearby information. The nearby domain is determined by the kernel function  $W$ . The kernel approximation can be expressed by the following equations,

$$\langle f(\mathbf{x}) \rangle = \int_{\Omega} f(\mathbf{x}') W(\mathbf{x} - \mathbf{x}', h) d\mathbf{x}' \quad (1)$$

$$\langle \nabla \cdot f(\mathbf{x}) \rangle = \int_{\Omega} f(\mathbf{x}') \cdot \nabla W(\mathbf{x} - \mathbf{x}', h) d\mathbf{x}' \quad (2)$$

where,  $h$  is the smoothing length which determines the size of the nearby domain also called influence domain or impact support. During this domain, the kernel function  $W$  should satisfy the conditions involving normalization(3), compact supportiveness(4), and Dirac delta property (5).

$$\int W(\mathbf{x} - \mathbf{x}', h) d\mathbf{x}' = 1 \quad (3)$$

$$\text{if } |\mathbf{x} - \mathbf{x}'| \leq kh, \quad W(\mathbf{x} - \mathbf{x}') \geq 0 \quad \text{else} \quad W(\mathbf{x} - \mathbf{x}') = 0 \quad (4)$$

$$\lim_{h \rightarrow 0} W(\mathbf{x} - \mathbf{x}', h) = \delta(\mathbf{x} - \mathbf{x}') \quad (5)$$

The next step is to discretize the above integral functions into the summations over particles in its influence domain. This step is called particles approximation, following with

$$\langle f(\mathbf{x}_i) \rangle = \sum_{j=1}^N \frac{m_j}{\rho_j} f(\mathbf{x}_j) W(\mathbf{x}_i - \mathbf{x}_j, h) \quad (6)$$

$$\langle \nabla \cdot f(\mathbf{x}_i) \rangle = - \sum_{j=1}^N \frac{m_j}{\rho_i} f(\mathbf{x}_j) \cdot \nabla W(\mathbf{x}_i - \mathbf{x}_j, h) \quad (7)$$

According to the above process involving kernel and particle approximations, it is managed that derive SPH formulations for partial differential equations governing the physics of solids.

### 2.2. Improvements for standard SPH

Although SPH has been applied to different engineering problems, it still suffers some drawbacks like inconsistency on the boundary, zero-

mode problems, and various numerical instabilities. Particularly, in solid dynamics with large deformations, the numerical instabilities involving tensile instability and pairing instability are considerable problems that can lead to unphysical fractures. As a classical article discussing the SPH instability [26], studied the stability analysis of standard SPH and firstly proposed the important concept “tensile instability” which means particles severe clumping phenomenon in stretch sections of material. Tensile instability as a typical weakness for the application of SPH has been paid much attention to the development of SPH applications recently.

As one of the most common and easiest techniques to reduce the numerical oscillation, artificial viscosity (AV) term is added to momentum and energy conservation equations in SPH formulations proposed initially by Refs. [14,27,28], given by:

$$\prod_{ij} = \frac{-\alpha \bar{c}_{ij} \mu_{ij} + \beta \mu_{ij}^2}{\bar{\rho}_{ij}}, \quad \vec{v}_{ij} \cdot \vec{x}_{ij} < 0 \quad (8)$$

$$\mu_{ij} = \frac{\bar{h}_{ij} \vec{v}_{ij} \cdot \vec{x}_{ij}}{\left| \vec{x}_{ij} \right|^2 + \left( \kappa \bar{h}_{ij} \right)^2} \quad (9)$$

where  $\alpha$  and  $\beta$  are constants. The notations  $\bar{c}_{ij}$ ,  $\bar{\rho}_{ij}$  and  $\bar{h}_{ij}$  are the quantities average of particle  $i$  and  $j$ . When  $\vec{v}_{ij} \cdot \vec{x}_{ij} > 0$ ,  $\mu_{ij} = 0$ . Although artificial viscosity has been improved in several modified versions, it is still limited to ensure stability during SPH simulations, especially, during the material with large tension.

Artificial stress term was developed by Refs. [29,30] to specifically remove tensile instability in elastic dynamics. It is implemented by adding a strong repulsive force only when particles become too close to each other, resulting in a more stable simulation for elastic problems by SPH, but just for 2D problems. Corrective SPH (CSPH) proposed by Chen in Ref. [31] also targeted to address the tensile instability. The idea of this corrective method is to transfer the kernel estimate concept to the Taylor series expansion. Sugiura and Inutsuka [32] mitigate the tensile instability using the Godunov SPH method [33] that utilizes a Riemann solver and achieves the second-order accuracy in space. They conducted the linear stability analysis for the equations of the Godunov SPH method, and find that the tensile instability can be suppressed by selecting appropriate interpolation for density distribution in the equation of motion for the Godunov SPH method even in the case of elastic dynamics.

Above several improvements are completely based on the formulations of standard SPH where particles interact through a kernel function defined on the current configuration. According to the study in Ref. [34], it means that particles can enter or exit each other's support domains as the material deforms, which is maybe one of the reasons leading to tensile instability. Total lagrangian SPH developed recently calculated the kernel function on the reference configuration, which appears a good performance in removing tensile instability [35,36]. The doctoral thesis of Reveles [35] developed a total Lagrangian SPH code for solid dynamics and it seems at present one of the most promising approaches to keep the numerical stability when applied SPH to HVI

problems with quickly extreme deformations. Then, the pseudo-spring technique was developed particularly for modeling crack growth in impact problems [37–39], combined with SPH formulation (so-called Pseudo-spring SPH). An efficient immediate neighbor interaction was formulated by connecting neighbors through pseudo-springs in this technique. The damage of material is evaluated by the behavior of pseudo-springs, which seems a very interesting approach to investigate the crack propagation during impacts. There are also other forms of SPH improvements such as MLSPH [40,41], Godunov SPH [32,33],  $\delta$ -SPH [42], and Gamma-SPH [43] et al., all of which are developed under the motivation to different SPH applications. Fig. 1 lists the developments of SPHs in the past forty years, not involving all but including the most several important formats. More detailed reviews about developments of SPH formulations can be found in Refs. [20,44,45].

### 3. Application in dynamic solids

The SPH method has been applied for solid mechanics problems since the early 1990s - [53,54]. Manipulated its particle discretization with much flexibility to track the material movement, some success has been acquired in the simulations performed by SPH methods for solids undergoing very large deformations, like high-velocity impact problems. This section mainly introduces the implementation of SPH formulation in HVI problems.

#### 3.1. HVI problem description

The response of structures under high-velocity impact loading is complicated and uncertain, which depends on the material properties and impact conditions including projectile shapes, deformable or rigid projectile, impact velocity, target configuration particularly the thickness, and target materials [25]. classified the most frequent types of damages during HVI for thin or intermediate targets, as shown in Fig. 2. All of these damages result from the initial compression wave and they often happen with more than one single form in specific impacts, which often involve the elastic-plastic deformation, shear deformation, hydrodynamic process, phase transition, etc.

This study aims to review the SPH simulation on impact thin structure, and the definition of the thin structure has been given in the introduction. For the thin structure impacted by high velocity, the perforations accompanying plugging a), ductile hole enlargement b), radial fracture c), as well as fragmentation and debris cloud phenomenons d), as shown in Fig. 3, have been observed in many experiments. At the same time, the shapes of projectiles also determiner the mechanical damages during the HVIs, for example, the research by Ref. [39] which studied the influences on the perforation of metal targets impacted by different types of bullets, the simulation carried out by SPH framework. More importantly, the damage types considerably rely on the target properties like ductile plates, brittle plates, as well as advanced composite plates such as [55–58]. Particularly, for the brittle thin plates like the study in Ref. [59], the ejecta and debris environment was emphasized to be investigated during HVIs. Ceramic as a typical brittle material has been widely used as a target material in the various engineering

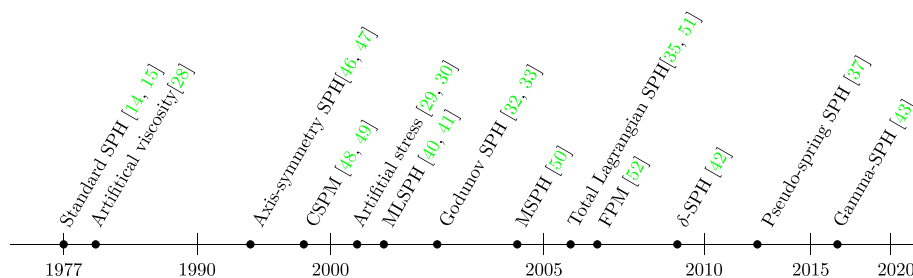


Fig. 1. Developments of SPHs [48,50,51].

## The mechanics of penetration of projectiles into targets

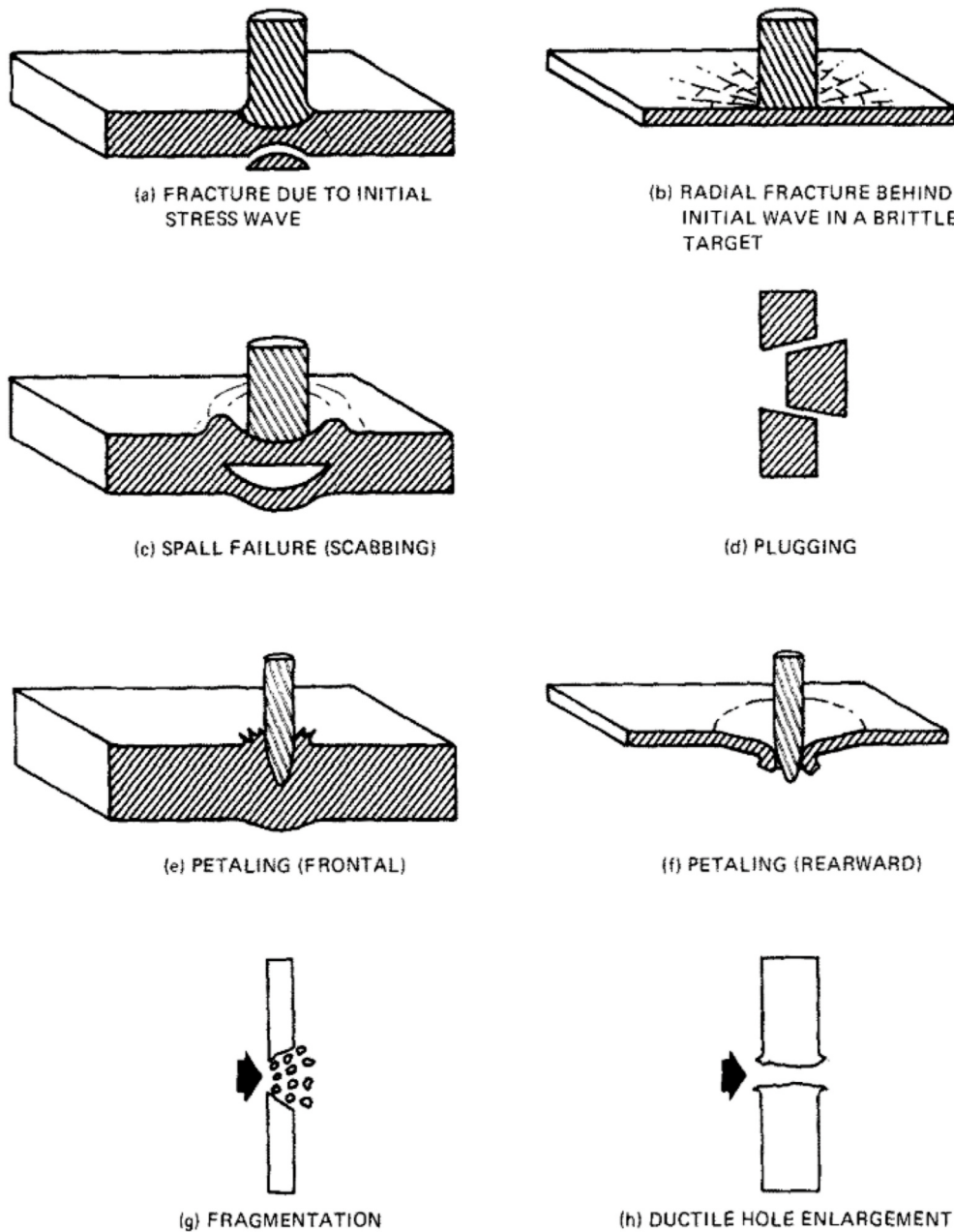


Fig. 2. The types of damages in HVI from Ref. [25].

environment. It also motivates that lots of research are developed to study the ceramic damage with fragmentation during the HVIs such as [60–63] by SPH method. However, in terms of the fragmentation and debris phenomenon, the numerical investigation by grid-based methods like FEM and FDM is no longer suitable and effective while the SPH method with particle modeling shows its advantage with more flexibility. The next section would provide more evidence from the literature. Table 3 represents the SPH method that has been extensively used to simulate the debris environment in HVIs.

Because of the complexity during HVIs, in the application of SPH modeling projectile-target systems, the choice of constitutive laws to model the plastic flow and damage behavior is one of the most important works. The specific choice should depend on the situations such as forms of the projectiles (deformed or non-deformed), considering certain physical phenomena (penetration limits, crack propagation, debris

clouds, etc.), and of course more predominantly the material properties. With the advanced materials employed in impacts recently, the complicated material constitutive law compatible with SPH formulas also become a new challenging work in the application of SPH method on HVIs.

### 3.2. Materials with strength with SPH

The application of the SPH method on simulation HVIs is based on the development of SPH formulation to solid material with strength. The first presentation of an SPH formulation for materials with strength was proposed by Ref. [53] which became the reference method for afterward research of SPH modeling solids. Based on the formulation of standard SPH, the first modification advanced took into account the edge defect mentioned by Refs. [67,68] by replacing the standard density

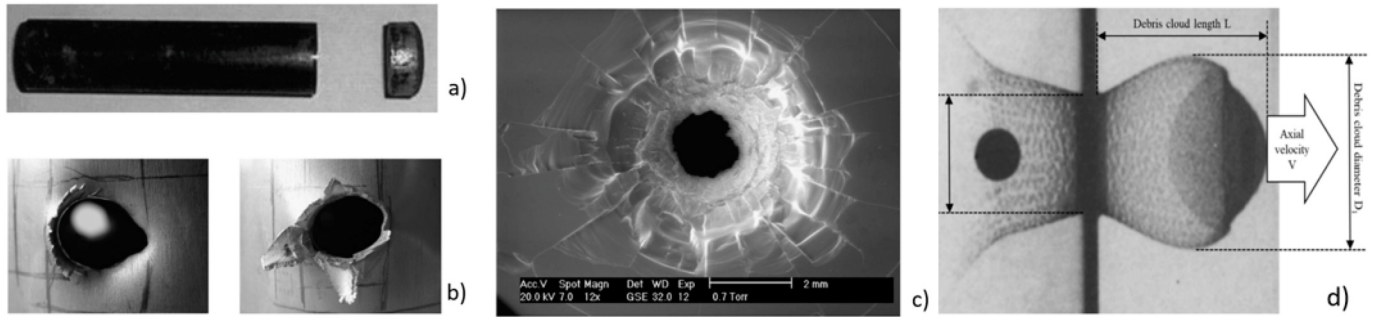


**Fig. 3.** The types of damages observed by HVI experiments: a) shows the plugging situation after perforation by Ref. [64]; b) shows the petaling and ductile hole enlargement after perforation by Ref. [65]; c) shows the perforation accompanying with radial fracture by Ref. [59]; d) shows the debris could during the impact by Ref. [66].

summation by a discretization form of the continuity equation:

$$D_i \rho_i - \rho_i \sum_j \frac{m_j}{\rho_j} \partial_{x_j^\alpha} W_{ij}^h v_{ij}^\alpha = 0. \quad (10)$$

The same procedure was also proposed by Ref. [69] and introduced a boundary term in momentum and energy equations. The next modification focused on material behavior and stress. Instead of using simply the hydrostatic pressure, they proposed to replace it by the complete stress tensor  $\sigma$  as follow:

$$(\text{momentum conservation}) D_i v_i^\alpha = \sum_j m_j \left( \frac{\sigma_i^{\alpha\beta}}{\rho_i^2} + \frac{\sigma_j^{\alpha\beta}}{\rho_j^2} + \Pi_{ij} \delta^{\alpha\beta} \right) \partial_{x_j^\beta} W_{ij}^h \quad (11)$$

$$(\text{energy conservation}) D_i u_i = -\frac{1}{2} \sum_j m_j \left( \frac{\sigma_i^{\alpha\beta}}{\rho_i^2} + \frac{\sigma_j^{\alpha\beta}}{\rho_j^2} + \frac{1}{2} \Pi_{ij} \right) (v_i^\alpha - v_j^\alpha) \partial_{x_j^\beta} W_{ij}^h \quad (12)$$

where the stress tensor is decomposed into a spherical part and a deviatoric part:

$$\sigma^{\alpha\beta} = -P \delta^{\alpha\beta} + S^{\alpha\beta} \quad (13)$$

where,  $P$  is pressure and  $S^{\alpha\beta}$  is the deviatoric stress tensor. The deviatoric stress tensor  $S^{\alpha\beta}$  can be calculated by its derivative,

$$\frac{dS^{\alpha\beta}}{dt} = 2\mu \left( \dot{\epsilon}^{\alpha\beta} - \frac{1}{3} \delta^{\alpha\beta} \dot{\epsilon}^{\gamma\gamma} \right) + S^{\alpha\gamma} R^{\beta\gamma} + S^{\beta\gamma} R^{\alpha\gamma} \quad (14)$$

$$\dot{\epsilon}^{\alpha\beta} = \frac{1}{2} \left( \frac{\partial v^\alpha}{\partial x^\beta} + \frac{\partial v^\beta}{\partial x^\alpha} \right) \quad (15)$$

$$R^{\alpha\beta} = \frac{1}{2} \left( \frac{\partial v^\alpha}{\partial x^\beta} - \frac{\partial v^\beta}{\partial x^\alpha} \right) \quad (16)$$

Combined with the SPH formulations, equations (14)–(16) can be described as summation forms of particles by following formula:

$$\left( \frac{\partial v^\alpha}{\partial x^\beta} \right)_i = - \sum_{j=1}^N \frac{m_j}{\rho_j} (v_i^\alpha - v_j^\alpha) \frac{\partial W_{ij}}{\partial x_i^\beta} \quad (17)$$

### 3.3. Material constitutive laws

Various material models have been used in the SPH method for solid structures, the elastic-plastic models like the Johnson-Cook (J-C) model [70] are most commonly used among the metallic projectile-target systems. In the beginning, an elastic-perfectly-plastic model was applied in most research like [54,71]. For the perfectly-plastic model, the Von Mises yield criterion was used often. The second stress invariant  $J_2 = 0.5 S^{\alpha\beta} S^{\alpha\beta}$  is checked in every time step. If  $\sqrt{J_2}$  exceeds the yield stress  $\sigma_y/\sqrt{3}$ , the individual stress components are given new values

$S_{new}^{\alpha\beta} = f S^{\alpha\beta}$ , where the value of  $f$  is defined by

$$f = \min \left( \frac{\sigma_y}{\sqrt{3 J_2}}, 1 \right) \quad (18)$$

The Johnson-Cook (JC) model includes a high strain rate, large strain, and temperature effects, which initially proposed by Ref. [70]. The yield stress is no longer predetermined as a constant like the perfectly-plastic model, and is replaced by the following equation:

$$\sigma_y = \left( a + b \epsilon_p^n \right) \left( 1 + c \ln \left( \frac{\dot{\epsilon}}{\dot{\epsilon}_0} \right) \right) (1 - T^{*m}) \quad (19)$$

where, the parameters  $a, b, c, n$  are constants related to material properties.  $\epsilon_p$  is the plastic strain and  $\dot{\epsilon}$  is plastic strain rate.  $T^* = \frac{T - T_{room}}{T_M - T_{room}}$ , where  $T_M$  is the fictitious melting temperature of the material,  $T$  being the current temperature,  $T_{room}$  being the room temperature and  $m$  being the thermal softening exponent. This model has widely applied in predicting the failure process of ductile materials under impact loading.

The constitutive laws have a significant influence on simulation accuracy. Therefore [72], developed a modified Johnson-Cook (MJC) model focusing on strain rate and adiabatic heating effects to investigate the response of steel and aluminum alloy plates impacted by projectiles with various geometries involving blunt, conical and ogival noses. The simulations were performed by the SPH method. Additionally [39], studied the effects of six different damage models on the computed ballistic response of metal plates (Weldox 460E steel and 2024-T351 aluminum alloy plates). They included Wilkins, maximum shear stress, constant fracture strain, Cockcroft-Latham, Johnson-Cook, and Bao-Wierzbicki fracture models.

In recent years, the types of material applied in projectile-target systems trend to be diverse because of the engineering requirements. Some brittle materials like ceramics and optical glass, and advanced composites often are employed as target plates in impact structures, suffering the large pressures, shear strain, and high strain rates. The more suitable constitutive laws for these materials also should be developed and implemented in the SPH method. For example, Johnson-Holmquist 2 (JH-2) model developed by Ref. [73] is a good choice for the brittle materials [60,74]. [62] investigated the behaviors of ceramic and ceramic-metal composite plates under impact by the SPH method, and they mainly compared the performances of three constitutive models JH1, JH2, and JHB applied to the target material.

Also, for the projectile-target systems with composite laminate targets, the more complicated constitutive laws and combination with SPH formulations should be reconsidered. The research like [55–58,75,76] incorporated the different material behavior laws to investigate the responses of composite laminates under impacts [55]. used an orthotropic elastic-plastic constitutive law in the SPH and predicted the perforation of graphite/epoxy (Gr/Ep) laminates [75]. employed a one-parameter visco-plasticity composite material model to a laminate with eight

Gr/Ep layers and investigated the effects of the strain-rate dependency on the perforated area under impacts. The constitutive equation of orthotropic fiber-reinforced composites combined with a self-defined failure model was used by Ref. [57] to study the impact response of Carbon fiber reinforced plastics (CFRPs) target by SPH method. The self-defined failure model involved damage criterion considering the orthotropic nature of each ply and material degradation rules considering microscopic damage and stress transfer mechanisms. In terms of specific composite materials, the first challenging is to develop effective constitutive law and the other is implemented into the SPH method. Table 3 represents the state of the art on SPH simulations of HVI problems, which involves the material law applied for projectile-target systems in the literature.

#### 4. SPH modeling impact process: a state of the art

To apply a numerical approach to specific engineering problems, it consists of three parts: (1) the objectives to investigate certain physical phenomena; (2) development of the material models such as constitutive laws and damaged models; (3) the compatibility between numerical formulations and material equations. This section mainly provides a state of the art about SPH application in High-velocity impact problems in the past 30 years. The statement is also represented from these three points. Firstly, an introduction about the initial developments of SPH codes in the 90s is provided combined with the HVI application. As the SPH codes were increasingly improved, they were incorporated into some commercial CAE software like LS-DYNA, Abaqus, and Hyperworks. More HVI simulations were performed by SPH solvers in these kinds of software, particularly, in LS-DYNA. With growing attention to the potential of SPH simulating solid dynamics involving large deformations, the good compatibility of SPH formulations encourages some coupled methods using the SPH algorithm combined with other numerical methods like mesh-based or some statistics approaches. The HVI simulations performed in these new frameworks are also summarized after. Lastly, some HVI examples deducted by SPH methods involving advanced materials like composites are also reviewed.

##### 4.1. First proposal - 1990

The first application dedicated to Hight Velocity Impacts on structures by the use of the SPH method seems to appear in the early 90s from one side by Ref. [77] and from the other side by Ref. [78]. A few years earlier [79], had introduced a particle method named NARBOR nodes to model violent impacts. This grid-less method uses the idea of neighbor particle interactions to define simplified strain and stress fields in a Lagrangian frame. This procedure based on free-nodes allows variable nodes connectivities and thus to deal with severe distortions. This first approach had given the inspiration that particle methods can offer interesting tools to investigate such complex situations.

In 1990, at the Next Free-Lagrange Conference, both [77,78] have exhibited a very similar work [78] introduced a very common standard formulation based on the work of [27,67] which discretized the Euler's equations associated with a Tillotson EOS to model shocks, expansion, and change of phase of metals, such as Iron in this case. As firstly introduced by Ref. [27], in the presence of shock waves to prevent inter-penetration and spurious oscillations, an artificial viscosity had been introduced in the momentum and energy equations. The numerical test introduced in this study corresponded to the case of an Iron disk of 0.6 cm thickness and a 2.1 cm radius impacted at 6 km/s by an Iron sphere. The radius of the projectile was not given but seemed to be very close to the target thickness of 0.6 cm. The two bodies were discretized with 1984 particles for the target and 192 particles for the projectiles, distributed randomly. This work did not show any strong validation, although it compared, without showing any support of this, the SPH result with a Finite Difference result. Only some shape differences and dimensions were displayed, which suggested that the SPH procedure

could offer a "realistic" solution for HVI problems at that age.

Subsequently [78], provided the encouraging results by the SPH method in applied impacts. And more worthy, this study pointed out the important limitations such as: running time where he suggested the use of parallel computation; reducing shocks smoothing and inter-penetration; the implementation of physical phenomena such as surface tension, viscosity, and material strength; treatment of boundary conditions; optimal kernel and h-value because he used a Gaussian kernel. On the other side [77], presented the code-named SPHC which seemed to be very similar to the one proposed by Ref. [78] at the difference that the SPHC code used two-dimensional Cartesian modeling and employed a Mie-Gruneisen EOS. The validation test consisted of an aluminum cylinder impacting an Aluminum plate at a speed of 7 km/s. The dimensions of the projectile and the plate were not given but should be in the same order as the previous test. Very few information was given except for the fact that the whole model was discretized with 500 particles. Again, no validation was presented, only the shape of the deformed target was discussed. These two works are the very beginning of HVI SPH modeling and even if no true validation is presented, both could conclude that the SPH method is very appealing for its simplicity and its capability to model important material distortions.

In the SPH models provided by both Cloutman [78] and Stellingwerf [77] at that time, they used the same standard formulation by considering only the Euler's equations with symmetric SPH discretization including an artificial viscosity. Particularly, at that age, the density evolution was not governed by the continuity equation but instead by the density summation:

$$\rho^h = \sum_j W_{ij}^h m_j. \quad (20)$$

Such a model provided a quite stable way to model perforation of structures for very high-velocity impacts as it can be observed with Fig. 4. It involved symmetrical SPH discretization of the linear momentum and energy conservation equations in the Euler's equations, employing linear and quadratic artificial viscosity, performed with the density summation procedure, and using an adapted time step. Nevertheless, at that stage the estimation of the method efficiency was not clearly revealed since no strong comparisons with experiments or other data have been brought.

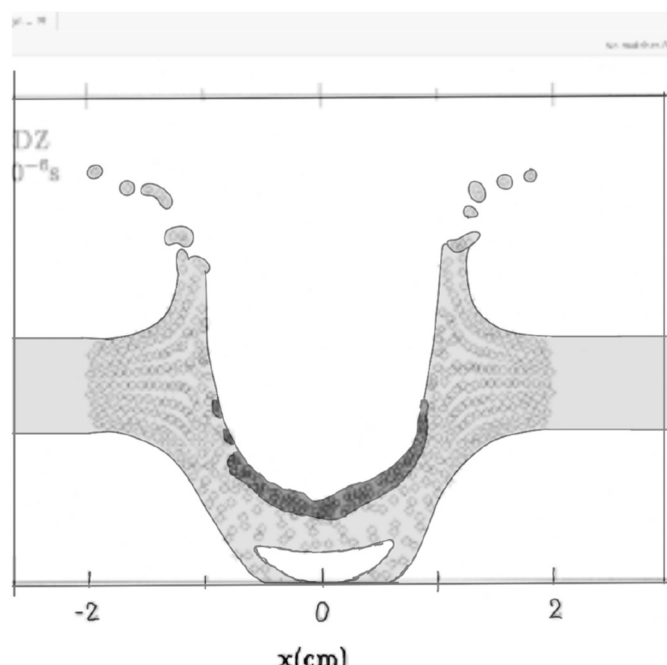


Fig. 4. Illustration of the Stellingwerf's test [77].

#### 4.2. Initial developments of SPH codes in HVIs

As one of the pioneers in developing the SPH modeling impact problems, Petschek et al. [54] developed a 3D standard SPH code involving the artificial viscosity by Monaghan [28] and simulated a 3-g copper disk (11.18 mm diameter x 3.45 mm thick) impact on a 2.87 mm thick aluminum bumper plate at 5.55 km/s. In this code, the Mie-Gruneisen equation with the von Mises criterion was applied to model the projectile and target material. Although a predetermined fixed value was given to describe the plastic flow regime during this high impact process, an encouraging result obtained by this code was that the maximum width and length of the debris clouds after impact were in agreement with experiments. Also, Stellingwerf is one of the pioneers in this field. At the beginning of the use of SPH method, Stellingwerf and his co-workers made a review of this computational technique in Ref. [71], and illustrated the great potential of this SPH method by the number of different simulations: a spherical aluminum projectile with radius 0.475 cm impacting a thin aluminum sheet with thickness 0.0381 cm at a velocity of 6.75 km/s, and including a series of impact simulations with disk projectiles radius of 0.95 cm impacting a 0.127 thick target at 10 km/s. The simulations were validated against published experimental data. The same group of researchers studied the variations in crater volume caused in the copper sphere impacts copper target with 4.0/3.0 cm thick at initial velocities from 6.0 km/s to 24.5 km/s using four numerical codes including SPH, MESA, EPIC and CALE codes in Ref. [80]. The investigation on the effect of a change in the yield strength in the material model was done and good agreement was found between these codes. In 1993, Johnson et al. incorporated SPH algorithm into a standard Lagrangian code such as EPIC in Ref. [81]. It modeled the copper rod impact steel plate with 2.6 cm thick at 2 km/s and 4 km/s, and copper rod impact aluminum plate with 12.7 cm thick at 5 km/s. The Mie-Gruneisen EOS and the constitutive model of Johnson and Cook (1983) were applied in these simulations. These studies involving the validations between SPH code simulations and experimental or other existing codes results made more and more researchers pay attention to the advantages of the SPH method in the application of HVI problems.

Except for EPIC software, SPH method was also incorporated into the other public numerical codes like AUTODYN-2D hydrocode and PAM-SHOCK 3D computer code. hayhurst et al. used an SPH capability implemented into the AUTODYN-2D software to simulate hypervelocity impacts on thin Whipple shield type target plates in 1997 [82]. The simulations included the impact of an aluminum sphere on aluminum plates with different thicknesses at around 6.8 km/s impact velocity, and a 6.35 mm-diameter sphere impacting normally on a 1.27 mm thick aluminum bumper at 7.22 km/s with the rear wall (a 3.175 mm thick aluminum plate) locating at 101.6 mm behind the bumper. The simulation debris cloud velocities and those measured experimentally matched each other within the range of measurable accuracy, which illustrated that SPH was a suitable way to investigate the debris cloud phenomenon in HVI. But, as authors commented that SPH still suffers from some significant weaknesses in some instability problems by Refs. [83,84]. In 1999, Faraud and his co-workers also investigated the debris cloud of the projectile impact on an all-aluminum triple wall system by the SPH method in Ref. [85]. The authors mainly compared the performances of two SPH formulations which had been incorporated into the PAM-SHOCK 3D computer code and the AUTODYN 2D hydrocode. Different constitutive laws were tested (Johnson-cook, Steinberg-Guinan), as well as different equations of states (Tillotson, Shock, Sesame). This study showed that the problems like shock pressure overestimation, not only emerged in the low-velocity impact simulations but also presented in the hypervelocity simulations at early stages of impact. Both the SPH codes achieved a good representation of the debris cloud expansion before the impact on the 2nd BS, but the simulations of the impact on the 2nd BS and BW could not agree with the experimental observations. Both the PAM-SHOCK 3D computer code

and the AUTODYN 2D hydrocode existed severe problems in energy and momentum conservation. Therefore, this study showed that at that age, the SPH technique was not sufficiently mature to support the development of complex debris shielding systems.

Hiermaier et al. in Ref. [86] and Groenenboom et al. in Ref. [87] also developed SPH codes and applied it to simulate HVI problem. The simulations were deformed by 2D SPH code, which concluded a 0.5 cm diameters Al projectiles impact 0.15–0.4 cm thick plates at 5.75–6.85 km/s in Ref. [86]. [87] conducted HVI both in 3D and 2D plane strain, investigating the role of a constant or variable smoothing length in SPH kernels, as well as the type of equation of state. The configuration involved a 4 mm diameter aluminum sphere impacting a triple aluminum with 0.8 and 3.2 mm thick bumper shield at 8 km/s. oblique tests were also conducted using 0.95 diameter aluminum spheres impacting a Whipple shield with variable thicknesses up to 0.3175 cm, at 6.78 km/s at 60° obliquity. The computed shapes of craters and debris clouds were compared to experimental data, illustrating the efficiency of the implementation of SPH for HVI for solid materials.

Actually, the SPH method obtained less interest and attention in the application of solid dynamics until the 21st century. The incorporation of SPH formulations to LS-DYNA commercial software provides much convenience to simulate HVI problems using this approach.

For example [59], used the SPH model in LS-DYNA to study the damaging and fragmenting processes during HVI on thin brittle targets. The simulation by the SPH model consisted of the steel projectiles on brittle targets (fused silica plates) of 2 mm thickness with velocity impact ranging from 1 to 4 km/s. The Johnson Holmquist material model and pressure cut-off criteria were chosen for target material. This SPH model successfully predicted the fragments clouds geometries and velocities. Besides, the perforation hole and spallation zones in the target were obtained in the simulation results, being in a good agreement with experimental observations. The influence of target thickness on damages and matter ejection was also investigated numerically in this study. Fig. 5 is the simulation result from Ref. [59], showing the spalling phenomenon, the particle clustering representing the macro and micro spalls naturally.

Kilic et al. performed perforation tests on 9 and 20 mm thickness armor by both Lagrange and SPH methods in LS-DYNA in order to determine the ballistic limit of 500 HB armor steel against 7.62 mm 54R B32 API hardened steel core ammunition in Ref. [88]. Johnson-Cook constitutive relations for both strength and failure models were developed in these tests. It is worthy to notice that, as concluded by authors in this study, the use of SPH formulation did not predict spall and fragmentation behavior more accurately as expected, even involving a finer particle size in the SPH discretization. What is worse, even a hybrid SPH modeling used to decrease numerical cost, still, SPH is too costly when compared with the Lagrangian formulation.

A series of experiments about cylindrical Lexan projectiles impact on steel target plates with a velocity range of 4.5–6.0 km/s were performed in the study of [89]. The authors also developed numerical models to these impact by SPH in LS-DYNA and the Eulerian-based hydrocode CTH, involving that a 2-D axisymmetric SPH model for both projectiles (5.58 mm diameter and 8.61 mm length) and target plates (12.7 mm thick) using a 0.05 mm distance between each particles. A combination of Mie-Grüneisen EOS and Johnson-Cook relationship was chosen for material modelling. The study compared numerical results to experimental data in terms of impact cratering and bulge, and demonstrated that both simulation models were in general agreement with the experiments capturing all the major features observed experimentally. As a further research by this same group, Roy et al. in Ref. [90] mainly optimized the numerical settings in these two simulation models, including determining SPH particle sensitivity, and identifying the best meshing strategy in CTH. The Hugoniot elastic limit and spall strength of A36 steel was mainly investigated combined the experimental and numerical results. Consequently, both simulation approaches SPH and CTH were proved to be able to accurately match the physical measurements of

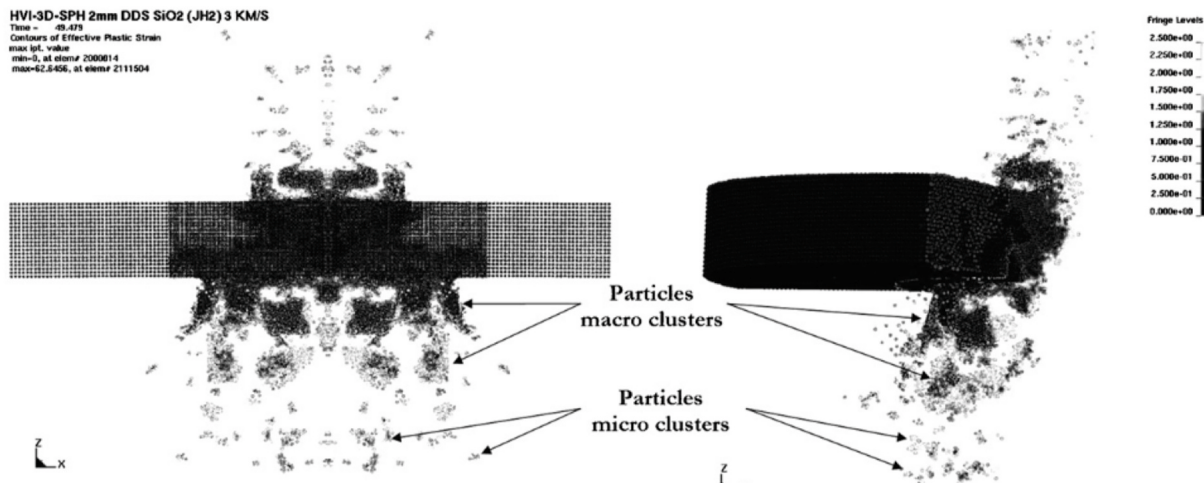


**Fig. 5.** Illustration of SPH simulation by Ref. [59]: two types of spalls can be identified (macro and micro spalls) represented by SPH particles clusters as fragments.

impact cratering, as well as predicting the velocity profiles in the PDV experiments.

Also, Xiao et al. studied SPH simulations by LS-DYNA of the normal perforation of monolithic and layered Weldox 460 E steel targets with impact velocity in the range of 80–405.7 m/s and target thickness in the range of 2–12 mm in Ref. [91]. A coupled constitutive model of viscoplasticity and ductile damage developed by Ref. [92] was used to model the dynamic behaviors of the target material Weldox 460 E steel. The model included constitutive relation considering stain hardening, strain-rate hardening and temperature softening and defines a damage evolution based on a constitutive relation considering stain hardening, strain-rate hardening and temperature softening and defines a damage evolution based on a modified Johnson-Cook fracture strain model. This work mainly studied the effects of target thickness or number of layers for the ballistic resistance of monolithic targets and layered targets based on a series of simulation results. By employing the SPH formulation in LS-DYNA, Thurber et al. in Ref. [93] performed the simulations of 9.53 mm diameter aluminum spheres, impacting 2.33 mm thick aluminum plates. They mainly investigated the assumption that the responses of materials under severe loadings like HVI involve the principal fluid-like behavior of solids. Different material parameters were implemented in the Johnson-Cook model, as well as Mie-Grüneisen EOS to simulate different shades of aluminum targets.

In addition, Sakong et al. in Ref. [94] also used the SPH method in LS-DYNA to simulate HVI problems with different projectiles and thin plates (steel and aluminum), but the main contribution in this study is that the fragment distribution from the particle dispersion during the impacts was analyzed by using a clustering algorithm. The authors firstly represented the possibility of applying the machine learning algorithm on the result analysis of high-velocity impact. In this study, the simulations involving cylindrical or sphere projectiles impact to aluminum plates with mm-scale thickness at 2.15 or 6.64 km/s velocities were performed. The Johnson-Cook model and the Mie-Grüneisen equation of state were applied for material behavior. The effects of various parameters such as inter-particle distance, uniformity of particle spacing, smoothing length coefficient, and time step scale factor were investigated in the aspect of accuracy. This study predicted well the HVI process involving the residual velocity, hole diameter, and spalling diameter, debris clouds in the target plates. Besides, the threat of the fragment to a certain structure can be evaluated quantitatively, by employing the machine learning algorithm to analyze the trajectory similarity of the particles.

#### 4.3. Some new SPH frameworks applied in HVIs

Although some commercial software like LS-DYNA, Abaqus, as well as Hyperworks have included SPH solvers, most of them implemented the standard SPH formulations, a few coupled with some improved techniques like artificial viscosity, artificial stress or conservation smoothing approaches. Several new frameworks based on the SPH algorithm are still developed aiming to get more stable and accurate simulations for HVI problems, such as pseudo-spring SPH, KGC-SPH, Gamma-SPH,  $\gamma$ -SPH-ALE, and decoupled finite particle method (DFPM).

Pseudo-spring SPH was developed initially by Amit and chakraborty et al. in Refs. [37,95]. The main concept of the pseudo spring strategy can be represented by Fig. 6, in which SPH interaction is restricted only to the nearest neighboring particles through connecting pseudo-springs. This network of springs is supposed between all the interacting particles, and they do not provide any extra stiffness to the system. The function of these springs is to collect all the information about damage state of the material and hence a damage evolution law defines degradation of the inter-neighbor spring forces. The interactions between particles are dominated by a parameter  $f$ , defined as  $f_{ij} = 1 - D_{ij}$ , where  $D_{ij}$  is the accumulated damage in the pseudo-spring between the  $i - j$  particles pair.  $D_{ij}$  is defined as  $D_{ij} = 0.5(D_i + D_j)$ , where  $D_i$  and  $D_j$  are the damage parameters at the  $i$ th and  $j$ th particles respectively. Therefore, by evaluating the interaction factor  $f_{ij}$  when it reaches the critical value, this spring breaks. The breaking of spring denotes the formation of a crack and the corresponding disconnected particles represent the material body on either side of this newly formed crack surfaces. Therefore, this pseudo spring technique has a fundamental strength in modeling crack propagation. The same group of researchers furtherly applied this model to study crack propagation in the bi-material interface in Ref. [95], and to study ballistic sensitivity of pre-notch in the metallic beam in Ref. [96].

In 2017, Islam et al. used this pseudo spring strategy combined with SPH to study the failure of ductile material under impact loading in Ref. [38]. A series of impacts of a cylindrical projectile on plates with 8 mm and 10 mm were simulated in this study, the material both of projectiles and targets being Weldox 460 E steel. As well known, ductile material failure is much more complex including large plastic deformation, heat generation due to plastic work, material instability due to localization of plastic deformation, and the growth of microvoids leading to damage. The attempt of this study implied that this SPH based on the pseudo spring method is a very promising approach to model the complex damages in impacts. In the same year, Islam et al. employed the pseudo-spring SPH to investigate the damage in ceramic and

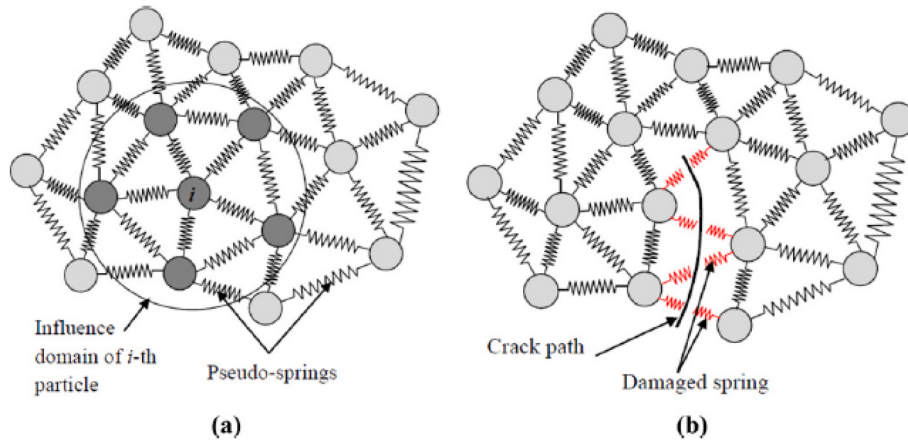


**Fig. 6.** The pseudo-spring model (a) undamaged configuration (b) cracked configuration from Ref. [37].

ceramic-metal composite structures under high impacts in citrachakraborty2017computational. The ceramics are typically brittle materials that involve abrupt failure and cracks, which is easier to be captured and modeled by use of the pseudo spring concept. Afterward, A Total Lagrangian SPH method was improved combined with Pseudo-spring contact by Ref. [97] to model crack initiation, propagation, and material failure of notched beams under the impact. This study provided several impact examples of notched beams, but no HVI simulations. Recently, Islam et al. in Ref. [39] used Pseudo-Spring SPH again modeling the projectiles impact metal target with a range of 6 mm–16mm thick plates. The projectile was modeled as a perfectly plastic material with very high yield stress (1900 MPa). The target was modeled by JC constitutive law, including usages of six damage models. This work mainly focused to investigate the effect of damage model on the computed ballistic response of metal plates (Weldox 460E steel and 2024-T351 aluminum alloy plates). The effects of the projectile geometry and hardening were also investigated in impact response. It can be concluded that the pseudo-spring SPH framework equipped with a suitable damage model can predict the plate perforation for different thick plates at different velocities. Moreover, in the same year, the authors in Ref. [62] used Pseudo-spring SPH to model ceramic and ceramic-metal composite plates including 30 mm deep target, 9 mm thin target, and deformed projectile. Three constitutive models JH1, JH2, and JHB were used in this study. Effects of interparticle spacing, the compact support of a kernel function, and types of kernel functions like the Wendland and the cubic B-spline kernels, as well as the projectile nose shapes (blunt, hemispherical and conical) on computed results have been described.

Zhang et al. in Ref. [98] developed an improved SPH called KGC-SPH (kernel gradient correction (KGC)) to model the impacts of an aluminum sphere penetrating an aluminum plate in two- and three-dimensional spaces. The KGC technique can mathematically improve the accuracy of the gradient of the kernel functions, which has been implemented to the SPH schemes both of 2D and 3D but only modeling the incompressible fluid flows [98]. firstly extended it to investigate the HVI process. In the KGC technique, a modified or corrected kernel gradient is obtained by multiplying the original kernel gradient with a local reversible matrix, and the detailed formulations can be found in Refs. [98,99]. The Johnson-Cook model and the Mie-Gruneisen eos were applied in the simulations. The simulations for 2D and 3D HVIs of 1.0 cm diameter aluminum cylinder onto a 0.4 cm thick aluminum plate at 6180 m/s and 4119 m/s were carried out. All the simulation results illustrated that the SPH method with KGC can be effective in modeling HVI problems and can produce more accurate results than the conventional SPH methods without kernel gradient correction. The followed work about the application of the SPH-KGC coupled method was provided by Ref. [100]. They mainly investigated the sizes of the craters

produced by HVI at different initial impact velocities and the variation of the crater size over the impact velocity. A series of 3D HVIs in which the aluminum sphere impacts the aluminum plate with a thickness of 0.4 cm at different velocities from 2 to 11 km/s (with an interval of 0.5 km/s) were performed and observed in this study. The two-stage phenomenon (the varying stage and steady stage during the increase of the crater size versus impact velocity) was accurately predicted by this new formula.

Limido et al. in Ref. [43] proposed an improved SPH called Gamma-SPH to reduce standard SPH drawbacks like lack of interpolation completeness, tensile instability, and the existence of spurious pressure, as well as high computational time. The main concept of this improvement is based on a centered formulation for the pressure gradient term in the momentum equation and on the introduction of a stabilization term proportional to the pressure difference between two neighbor particles. The stability of this new formulation is ensured and theoretically proved under a CFL-like condition. The simulations of 9.53 mm diameter aluminum sphere impact aluminum plates with 0.8 mm and 4.039 mm thick at 6.7 km/s velocity were conducted. Oblique impact consisting of a 3 mm aluminum sphere against to 2 mm thick aluminum plate at 32° tilted and 4059 m/s velocity was also simulated by this Gamma-SPH. The linear elastic-plastic material model along with the Mie-Gruneisen equations of state was used for material. The debris clouds for both normal and oblique impacts observed in simulation and experimental results were in good agreement. Besides, the authors also simulated the UNLV-1000-026 test which consists of a Lexan cylinder 5.6 mm diameter impact A36 steel 12.7 mm thick plate at 4.8 km/s velocity. Crater and spall zones were well replicated by GAMMA-SPH compared with experiments.

An alternative scheme called  $\gamma$ -SPH-ALE was developed to model the HVI cases and investigate the debris clouds in Ref. [101]. Indeed,  $\gamma$ -SPH-ALE is the combination of SPH-ALE formulation [102] and FV low-Mach scheme [103]. PDE is written in ALE formalism, allowing for a simple treatment of the arbitrary velocity field, ruling the particle motion. A stabilizing term extracted from the FV low-Mach scheme is also introduced using a velocity corrective term (depending on a parameter  $\gamma$ ). Proportional to the pressure gradient it improves the state variables evaluation. An artificial viscosity is combined with this  $\gamma$  velocity to ensure the global stability of the scheme. The simulations of aluminum spheres impact aluminum plates with different thick at 6.7 km/s were performed. And an oblique impact with a 3 mm-diameter sphere to the plate with 2 mm thick at velocity 4050 m/s was also deducted by  $\gamma$ -SPH-AL method. An elastic perfectly plastic material model combined with the Mie-Grüneisen equation of state was applied to the material of both projectiles and targets. The simulation results revealed that the proposed scheme increases both stability and accuracy, in reduced computation time, concerning classical solvers.

Zhang et al. also investigated the damaging effect of target plates induced by high-velocity impact using a decoupled finite particle method (DFPM) in Ref. [104]. DFPM was a recently developed corrective SPH method by Liu and his co-workers in Refs. [52,105]. DFPM does not need to solve redundant and challenging pointwise corrective matrix equations when approximating a field variable and its derivatives. The authors made a comparison on the formulations of different SPH improvements like FPM [105], CSPM [49] and KGC [98], and the point can be concluded that DFPM indeed has its advantages on mathematical accuracy and implementations. Different from these formulations of SPH versions like FPM, CSPM, and KGC all of them involving the corrective matrices which can be ill-conditioned in extremely deformed domains, DFPM can obtain a more stable calculation especially for cases with highly disordered particle distribution. Lots of 2D and 3D HVI examples including less than 5 mm thick metallic plates impacted by 2–13 km/s velocities were performed by both conventional SPH and DFPM in this study. The numerical results demonstrated that the DFPM can achieve a more accurate computation on the boundary than using conventional SPH, as well as have the capability to alleviate tensile instability. The hole size and damage in HVIs were also predicted and agreed with experimental data.

#### 4.4. Non-metallic projectile-target systems

Nowadays, environmental protection and safety standards in the modern industry make the materials of structures involving higher requirements, traditional metallic structures have been not enough. Some advanced structures like laminated composite structures are used in various engineering areas, involving aerospace, automotive, marine, civil, sport, etc. Generally, laminated composite structures include some properties such as high strength and stiffness to weight ratio, strong energy absorption, long fatigue life, good corrosion resistance, and often low production cost, contrasted to traditional isotropic structures. Because of this, more and more laminated structures are designed in engineering environments with severe loading impacts. The study of the dynamic response of impact laminated composite plates was also performed by the SPH method in recent years [55–58].

The differences in SPH modeling the targets with different materials can be shortened into two parts: one is the specific constitutive laws implemented into SPH formulations; the other is the modeling process by particles, particularly for laminated structures. The different constitutive laws for metals, various types of composite materials, as well as ceramics, have been developed and can be found in the literature. The challenging work is to integrate them into the SPH algorithms.

About modeling the laminated structures by SPH particles [56], introduced its details, as shown in Fig. 7. In this study, the authors used the improved SPH method to simulate an aluminum projectile striking to laminated graphite/epoxy (Gr/Ep) composite plate targets with several different layup configurations. Every single layer was modeled macroscopically as a uniform medium, and then the numerical laminated plate model for the SPH method realized the discontinuity of stresses between neighboring layers of the laminated composite plate targets. Fig. 7 illustrates this concept that the layers A and B are assumed to be arranged

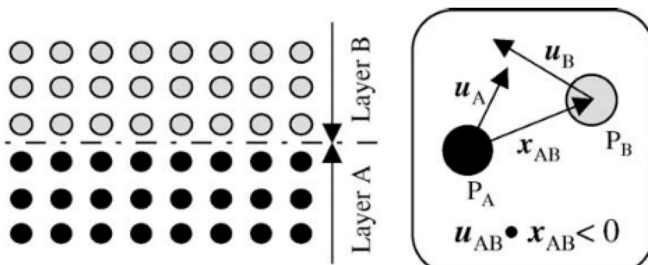


Fig. 7. Numerical laminated plate model by SPH particle from Ref. [56].

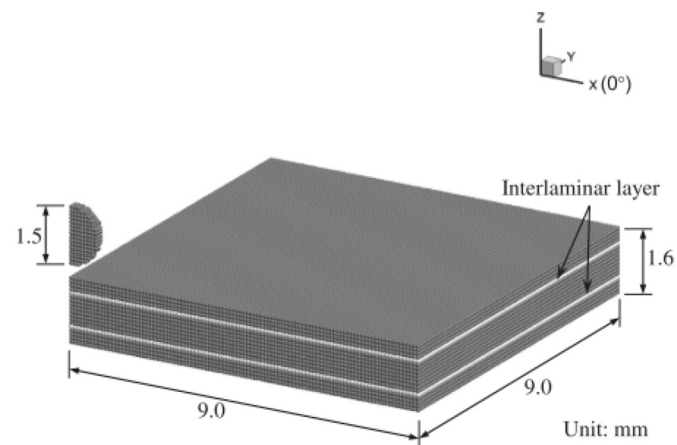
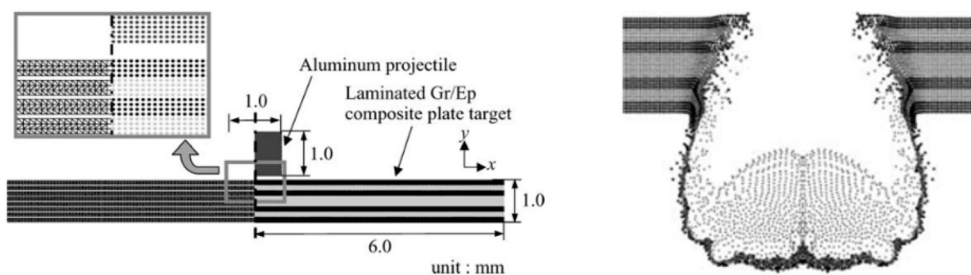


Fig. 8. The SPH model for CFRP laminate from Ref. [57].

without bonding. Then the model is based on the assumption that only positive pressure acts between the particles  $P_A$  and  $P_B$  which belong to layers A and B, respectively, when the two particles are approaching each other. The inner product of the relative velocity vector and the relative position vector of two particles is utilized to determine whether the two particles are approaching each other or not. Fig. 9 is the numerical model of the target in this SPH simulation. Back in the 1990s, the SPH method combined with the macro-homogeneous, anisotropic material concept for fiber composites was already developed for HVI problems by Ref. [55]. In recent years [57,58], etc. also employed a similar conception to model the laminated structures as the target in impacts (see Fig. 8).

Except for developing the SPH model for laminated structures, the main contribution in Ref. [56] is to develop an improved SPH method with new particle generation and particle merger techniques. The new particle generation technique means generating new particles if the area with no particles exceeds a certain value or the distance between the adjacent particles exceeds a certain value, following two rules. Because the new particle generation technique to prevent the numerical fractures causes the overabundance of particles. Another particle merger technique was presented in simulation in which two close particles of a triangular element are merged into one particle if the distance between the two particles attains a certain value. Fig. 10 displays a comparison with an HVI example between the results by standard SPH and this improved SPH. This improved SPH was proved not only a promising approach to decrease the numerical fracture during HVI problems involving the deformation with a large tensile strain by a conventional SPH, but also a robust and effective way to model the laminated plates.

Carbon fiber reinforced plastics (CFRPs) have good specific strength, specific modulus, and fatigue properties compared with conventional metals, so they have been applied to primary load-bearing structures such as wings and a fuselage in the latest airplanes. Yashiro et al. investigated mechanisms of the extension of high-velocity impact damage in CFRP laminates by experiments in Ref. [106] and numerical simulations with the SPH method in Ref. [57]. [[missingLabel]]8 shows the SPH model for a CFRP laminate, and the simulation in this study consisted of 1.5 mm diameter steel balls impact CFRP laminate with 1.6 mm thickness at 200–1200 m/s  $0^\circ$  and  $90^\circ$  layers for cross-ply laminate were modeled, as well as interlayer particles were inserted into the ply interface to represent delamination. Damage in a particle was judged by modified Chang-Chang criteria, and a material degradation rule was applied to the stiffness and stress in the damaged particle. This SPH model successfully predicted the high-velocity impact damage including a crater and matrix cracking/crushing in the top ply, catastrophic failure of the middle plies, and fiber breaks and matrix cracking in the bottom ply. In 2019, Giannaras et al. performed the simulations of carbon fiber reinforced polymer composites (CFRP) material behavior to



**Fig. 9.** The SPH model of the laminated Gr/Ep composite plate (left); debris cloud produced by impact at 4.0 km/s (right) provided in Ref. [56].

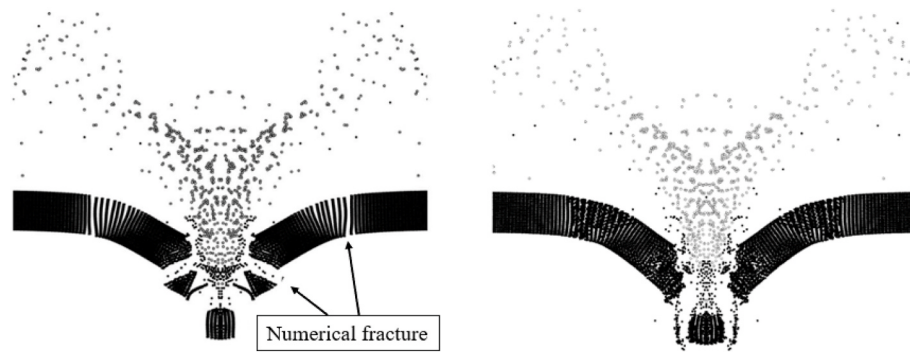


**Fig. 10.** The unphysical fractures during standard SPH model (left) and improved SPH model (right) in Ref. [56].

hypervelocity impact using the SPH model in LS-DYNA in Ref. [76]. The numerical examples consisted of the sphere projectiles with different diameters impact to 2.3 mm thick CFRP plates at the velocities ranging from 1.93 to 4.96 km/s. The simulation results including shapes of debris clouds, ballistic limit, and the crater diameters were in good agreement with experimental observations. It showed that the SPH method and MAT\_59 material model provided in LS-DYNA can predict the behavior of CFRP plates under the impact loading. However, the authors claimed that the numerical failures before material failure still should be alleviated by additional solutions. And a strain rate dependent and experimentally calibrated orthotropic material model should also be further developed to simulate CFRP behavior, which at the same time, should be compatible with the SPH code of LS-DYNA.

High-strength cementitious (HSC) materials also have been paid more attention in the application of passive protection from weapon effects recently, because of its properties involving comparatively low cost, ease of rapid on-site manufacture, and high early strength. Nor-dendale et al. studied the responses of the high-velocity projectile impact on HSC materials by both Traditional Lagrangian finite element analysis (FEA) and SPH in Ref. [58], and they mainly focused on a comparison of the simulation performances between FEA and SPH models. The projectile used was a MIL-P-46593A Standard fragment simulating projectile (FSP), and the HSC plates were modeled by a modified Advanced Fundamental Concrete (AFC) constitutive model in both FEA and SPH methods. Multiple impact simulations were performed with velocities varying from 1067 m/s to 1097 m/s. The authors concluded that the ability of the SPH model to capture residual velocity proved to be just as accurate as traditional FEA models, but they are significantly more time-consuming. However, SPH has a great advantage to model debris field compared to traditional FEM; and modeling the high-rate impact of a brittle target is the issue of spalling and fragmentation.

Ceramics as a typical brittle material are often used in protective structures, so the understanding of the performances of ceramic plates under high impact loading is also a significant work. The difference of SPH modeling ceramics target and metallic target in HVIs is mainly on the usage the suitable constitutive laws, which has mentioned in section

3. In 2020, a recent study was provided by Xiao et al. that SPH models were established to simulate fracture and fragmentation of the projectile and the target during the impact process of a ceramic tile by a projectile in Ref. [60]. The case of an  $\text{Al}_2\text{O}_3$  ceramic plate with 12.7 mm thickness impacted by a deformed cylinder with a diameter of 6.14 mm and a length of 20.86 mm at 903.9 m/s was conducted by SPH model in LS-DYNA. JH-2 model (Johnson and Holmquist (1994)) was used to describe material behaviors of  $\text{Al}_2\text{O}_3$  ceramic, which includes pressure, strain rate, damage, and bulking effects. The simulation result showed that the JH-2 model is suitable and attractive for modeling the high-velocity impact of ceramic-type materials. In this study, two methods including a penalty contact method (PCM) and particle approximate method (PAM) were employed to handle interactions between the projectile and the target. The simulation results illustrated that PCM and PAM induced insignificant differences in modeling the high-velocity impact of the deformable projectile on the ceramic tile. The sensitivity of SPH numerical parameters like artificial viscosity, smoothing length, and particle spacing on simulation results was also investigated.

Another new study by Ref. [63] is to develop an FE-SPH coupled model to investigate the responses of HVIs with the  $\text{Al}_2\text{O}_3$  tiles target and multilayer targets with  $\text{Al}_2\text{O}_3$  front layer and AA6061-T6 backing layer. In this model, the FE belonging to the ceramic part was converted into SPH particles when the element conversion criterion was met. Two projectiles were used:  $7.62 \times 51$  P80 and  $12.7 \times 99$  AP in the simulations. This study concluded that the FE model can not obtain accurately simulating the transmission of the projectile decelerating force to the rear plate with a consequently incorrect prediction of the residual velocity and damage morphology in multilayer targets. In contrast, the SPH model combined with FEM elements is more suited for the simulation of the response of ceramic materials. Fig. 11 is the numerical result of impact multilayer target, from which it can be seen that the crack is the principal damage for brittle ceramic plate. Indeed, as the above description of the new types of SPH schemes, ‘pseudo-spring’ SPH seems the most promising approach to simulate the ceramic damages under impact conditions because of its natural property to capture the crack transmission by the behavior of pseudo-spring [62].

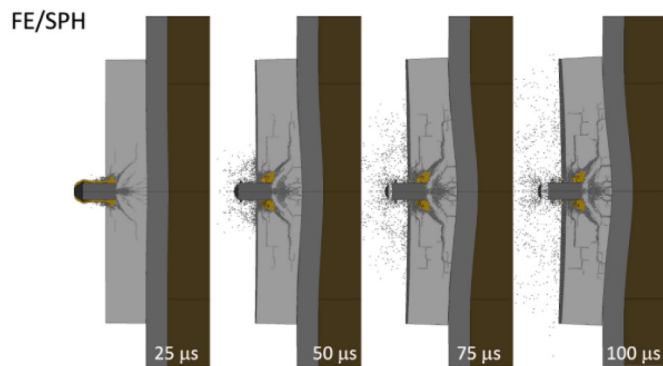


**Fig. 11.** Impact sequence of 7.62 × 51 P80 against multilayer target simulated by the numerical models from Ref. [63].

## 5. Limitations and improvements of using SPH for HVI modeling

Some advantages of the SPH method applied to simulate the dynamic solids have been well recognized, and from the literature review in the last section, it can be seen that this numerical method also has become one of the most important approaches to investigate the responses of high-velocity impacts. However, the pioneers warned about numerical weaknesses in the use of this mathematical formulation for solid mechanics. The shortcomings of SPH algorithm like estimated accuracy of neighbors, interfaces for large density discontinuity, high time-consuming, and the particles instabilities become more visible in modeling large solid structures. Particularly, the instabilities due to tensile behavior are inevitable in simulating solid dynamic problems like HVIs. In the earlier 1990s, some techniques including conservation smoothing by Ref. [107] in 1994, implementation of kernel renormalization by Refs. [47,108] in 1996, more accurate computation on the boundary by Refs. [69,109] had been developed to improve the SPH performances. The details are provided by the earlier review articles in Refs. [23,110]. With the motivation of simulating HVI problems that involve more complicated and uncertain physical phenomenon, some improvements for SPH formulations are still under research combined with the mechanical properties in HVIs. Besides, the fracture models merged into SPH formulas also should be developed to improve the realism of complete fragmentation during HVI, as claimed by Ref. [110]. This section mainly reviews some articles which provide SPH improvements during the HVI simulations.

### 5.1. Accuracy, instability

In simulation research, numerical accuracy is the primary consideration that relies on numerical stability to some degree, but numerical instability is still the inevitable problem for most numerical algorithms. In terms of SPH simulating HVI problems, the particles often suffer the severe clumping phenomenon when the materials are under extremely large deformations. Some analyses for the stability of the SPH method has been done by Belytschko and his co-workers based on the features of the particle method with Eulerian and Lagrangian kernels in Refs. [34, 111,112]. Several types of instabilities including tensile instability were identified, and they claimed that tensile instability is a severe limitation to the SPH application in solid dynamics. Artificial viscosity is the most common technique to mitigate the numerical oscillations, also to reduce tensile instability for some problems. The earliest standard SPH also involves an artificial viscosity proposed by Monaghan et al. and the equations are represented in section 2. Nevertheless, the performances of this artificial viscosity depend on the choice of parameters ( $\alpha, \beta$ ), and it easily makes the system over-dissipative if unsuitable parameters are used. Shaw et al. [113] discussed this point in detail and introduced a modified method to avoid choosing unsuitable parameters. There are also some studies focusing on the effects of artificial viscosity on the

simulation results for impact problems.

Back in 1996, Johnson et al. studied the effects of different artificial viscosities for the SPH method in Ref. [46]. The types of artificial viscosity developed by different authors are listed in Table 1. Johnson et al. used five examples elected to describe a wide range of physical problems including plastic flow, wave propagation, erosion, rigid projector impact, and localized shear in this study. They were simulated by standard SPH formulations with six schemes of artificial viscosities, involving MAV by Monaghan al.et. in Refs. [14,27,28], BAL by Balsara et al. [84], node and bond viscosity [114], as well as three different combinations of parameters in MAV viscosity. By analyzing the simulation results, the authors declared that only changing the coefficients of MAV-type artificial viscosity can not provide improved results. Additionally, the types of artificial viscosity illustrated different performances for different problems. For example, the MAV-type viscosity showed generally good results in plastic flow, rigid projector impact, and wave propagation problems but appeared severe numerical instability in the other two examples. It is difficult to find that a certain existing artificial viscosity algorithm or set of coefficients was clearly superior for the range of problems. The conclusion of this study was only to remind users should pay much caution when performing SPH computations for specific problems. At the same time, more work was required to develop artificial viscosity algorithms (or other algorithms) to improve the SPH instability problem (see Table 2).

The smoothing length ( $h$ ) of kernel function and distance ( $d$ ) between particles are also important parameters that can significantly affect the stability of simulation results. The study by Mehra et al. in Ref. [116] considered this point and also investigated the influence of four SPH schemes including three types of artificial viscosity (MAV, BAL, and MON in Table 1) and a contact SPH scheme (CON) for the simulations of impact problems. They conducted a series of simulations on HVIs with variable values of the ratio  $h/d$ . The simulations consisted of the high-velocity impact of the metal sphere on thin metallic plates in 2D and 3D configurations. The Mie-Gruneisen and HOM equation of states were used in the simulations, coupled with the Steinberg-Guinan model for the strain and temperature dependence of the shear modulus and yield strength. The diameters of craters and shapes of the debris clouds achieved in the simulations were observed and compared with experiments. The authors discovered that both BAL and MON viscosities had a good performance for hypervelocity impacts, but the MAV viscosity and CON scheme can not obtain the correct debris cloud shape as measured even adjusted a wide range of  $h/d$ . However, it is worthy to notice that the CON algorithm (also called the Godunov-type scheme) with its attractive quality of being free from arbitrary parameters, performed well at moderate impact velocities, not suffering from the numerical fracture. So, there is still no existing artificial viscosity term which is capable to keep generalized stability for SPH simulations, especially for the HVI problems with complex physical responses.

Actually, in the SPH method, tensile instability is still the most unmanageable problem. When particles are under tensile stress state or sufficiently close to one another, the motion of the particles becomes unstable, which may lead to particle clumpings representing as large tension exhibit ‘numerical fracture’ or artificial void in structure. This situation becomes a more significant concern in impact and penetration

**Table 1**  
The types of artificial viscosity incorporated to SPH formulations.

Authors and Ref	year	abbreviation	parameters	description
Monaghan et al. [14,27,28]	1977	MAV	$\alpha, \beta$	The most common type, not stable
Balsara et al. [84]	1995	BAL	$\alpha, \beta$	capable for High-velocity impact
Vonnewmann et al. [114]	1950	NBAV	$\alpha, \beta$	not stable
Morris and Monaghan [115]	1977	MON	$\alpha^*$	capable for High-velocity impact

**Table 2**

The techniques incorporated to SPH formulations to mitigate tensile instability.

Authors and Ref	year	name	description
Monaghan et al. [29,30]	2000	artificial stress	capable for 2D and low-velocity impact in [29]
Parshikov et al. [33,121,122]	2000	Godunov-type scheme (CON)	capable for moderate/high-velocity impact (up to 3.1 km/s) in [116,119,120]
Reveles et al. [35,36]	2007	Total Lagrangian SPH	no much application in HVIs
Liu, Zhang et al. [52,105]	2006	(DFPM)	capable for High-velocity impact (up to 6 km/s) in [104]

problems since the elastic dynamics involve considerable attractive forces. In 2012, Liu and his co-workers [72] used the coupled SPH-FEM (SFM) to simulate high velocity perforation of steel and aluminum alloy plates of different thicknesses impacted by steel projectiles with various geometries, such as blunt, conical and ogival noses. The main contribution in this study is that a modified Johnson–Cook (MJC) model focusing on strain rate and adiabatic heating effects was adopted for metals, and material properties for Weldox 460E steel and AA5083-H116 aluminum plates were determined in the simulations. The authors claimed that for thin plates, due to the inherent tensile instability problem associated with the SFM approach, the agreement between numerical and experimental results was not obtained. Therefore, as introduced in section 2.2, most of the attention to improve the SPH application in solid dynamics is paid on the tensile instability problem.

Artificial stress also called Monaghan stress was the earliest technique to be particularized for solving tensile problems in solid dynamics in Refs. [29,30]. A strong repulsive force is added to momentum and energy conservation equations, only when particles become too close to each other. It has been validated in impact problems by Monaghan's research, but only performed for low-velocity impact problems. This artificial stress method was implemented into an axisymmetric SPH (ASPH) in the study of [117] to simulate the long ogive-nose steel projectiles impact into 26.3 mm thick aluminum targets. 2D axisymmetric SPHs are useful for normal penetration analysis because they can give equivalent results while reducing computational cost largely compared with a 3D SPH method [118]. But ASPHs often suffer from the problem of virtual tensile stresses and shear stresses at the projectile-target interface. The authors in Ref. [117] employed a particle-to-particle contact algorithm to treat contact interfaces and combined with this artificial stress approach to treat tensile instability. The numerical residual velocities showed very good agreement with the experimental observations and the tensile instability was also eliminated during the deformations. According to the study by Mehra et al., in 2012 [119], artificial stress could reduce the void size caused by particle tensile instability but unable to completely remove it when the impact velocity is high. Mehra et al. deducted simulations consisting of a steel sphere impact a 2 mm thick Aluminium plate at 3.1 km/s by SPH code combined with artificial stress and Godunov-type scheme (CON) in Mehra2012. The numerical results showed that the Godunov-type scheme (CON) performed better than artificial stress in terms of mitigating tensile instability. But this observation is only by one impact. As the authors claimed, more studies with different impact scenarios should be considered to identify the presence or absence of tensile instability in the Godunov-type SPH. In fact, Godunov SPH method was developed to remove the tensile instability initially applied in fluid dynamics, which uses a Riemann solver and achieves the second-order accuracy in space by Refs. [32,33]. In 2017, Sugiura et al. in Ref. [120] extended the Godunov SPH method to elastic dynamics by incorporating deviatoric stress tensor that represents the stress for shear deformation or anisotropic compression. The authors validated this algorithm in several classic examples such as the collision of rubber rings, oscillation of plate, as well as the impact problems. But, the impact example was still at

moderate impact velocities (3.1 km/s), and its performance is still unknown at high-velocity impacts. Total Lagrangian SPH is a new scheme which is validated that capable of removing the tensile instability, but there is no apparent examples on HVIs. Table 1 shows several approaches corresponded to impacts.

### 5.2. Time-consuming, coupled SPH, contact algorithms

Essentially, in SPH formulas, the approximation process is determined based on a contemporary domain of arbitrarily distributed particles, so neighbor searching is one of the most important steps in SPH to seek the nearest neighbor particles of a particle to define nodal connectivity. This directly leads to the SPH process time-consuming, especially for larger-scale and 3D problems requiring tremendous particles. To address this problem, two ways have been considered in the literature. One is employing the CPU/GPU computer algorithms, and the other is by coupling the FEM element model. A few studies like [123–125] have achieved the SPH formulation incorporated with GPU algorithms. Particularly, one work by Frissane et al. in Ref. [125] deserving to be mentioned is that a 3D SPH code linked with the GPU algorithm was developed to model the process of high-velocity impacts of thin metal plates struck by a blunt projectile. The simulation results showed that this 3D SPH GPU numerical code was able to accurately predict the response of HVI problems, more importantly, costing a restrained amount on calculating memory and time.

The SPH has a strong ability to solve dynamic problems with large deformations without mesh distortions while it is not as good as the FEM in terms of computational time and boundary conditions. Besides, FEM has been developed for many years and has been a very mature technique involved in different commercial software. With this concern, the coupled SPH-FEM method can effectively use the strengths of these two methods for the simulations of large deformation problems. Some studies focusing on the coupling algorithms also have been developed in the past years such as [121,122,126–129]. The coupled ways between SPH and FEM methods are mainly identified into two kinds: one way is converting techniques from FE elements to the SPH particles depending on the physical states of materials; the other is modeling different domains of the structure with SPH and FE respectively based on the interface contact algorithms. Fig. 12 shows these interactions between SPH particles and FEM elements. The left one is from the study of [130], which displays that all the structure is modeled by FEM elements at the beginning and then the elements convert to SPH particles as the material deforms increasingly. The right form is provided by Ref. [131], where the center part of the target plate existing large deformation is modeled with SPH particles and the other part with finite elements. Also, if the projectiles are deformed largely such as using brittle materials, they are modeled using SPH particles while elements for rigid or small performed projectiles.

An approach to couple FE-SPH methods is based on a Lagrangian mesh whose elements are converted into SPH particles when a conversion variable (strain, stress, or any state variable) reaches a critical value. This idea was proposed and applied to simulate impact problems initially by Johnson et al. [130,132,133]. In the study of [132], two different converting schemes were used: SPH nodes sliding on a standard finite element mesh and SPH nodes automatically generated from a standard FE mesh. The simulations were carried out by this coupled method involving rigidly pointed and rounded nose projectile impacting aluminum targets, as well as, tungsten penetrator impacting steel target. The same researcher group improved the converting technique based on setting mass nodes and stress points in Ref. [130]. A new coupled FE-SPH method called combined particle-element method (CPEM) was developed to model the process of HVI examples in this study. The oblique impact consisting of a steel rod impact 4340 steel plate at 2 km/s was conducted by this CPEM. Subsequently, Rodriguez et al. also applied this CPEM method modeling 4 mm-thick plate of aluminum impacted by the projectiles with different nose shapes (conical,

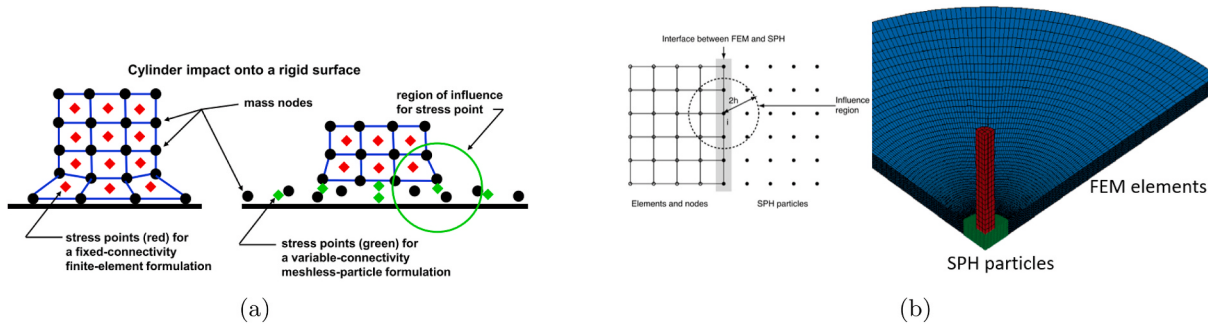


**Fig. 12.** The FE-SPH coupled models: Left is the elements converting to SPH particles as the material deforms increasingly from Ref. [130] and Right is modeling different domains of the structure with SPH and FE, respectively, from Ref. [131].

hemispherical, blunt) in Ref. [134]. It is proved that the coupled method can reduce the time-consuming compared single SPH modeling, as well as using the advantages of both FEM and SPH, but the implementation seems complex.

On the other hand, various contact algorithms are developed for calculating the contact interactions between SPH particles and FEM elements on the interfaces of FE-SPH domains. A contact algorithm based on a contact potential to link the SPH codes and FEM solver in DYNA3D (developed at Lawrence Livermore National Laboratories) is proposed in Ref. [135]. In this algorithm, FE nodes were treated as particles, then a particle to particle contact approach was applied, allowing frictionless sliding between FE and particles. The authors validated this FE-SPH coupled method by the simulations for three different impact problems: a plate impact, water impact, and rod penetration. The case of an ogive-nose high strength steel projectile impacting an aluminum plate under an angle of 30° was simulated, illustrating interesting results. As another example, an SPH-FEM coupling algorithm also was developed by Zhang et al. [136], which adopts background particles in the position of FE nodes, considering the attachment and contact between SPH particles and finite elements. The perforation of a cylindrical Arne tool steel projectile impacting a plate Weldox 460 E steel target was simulated in 3D at a series of impact velocities. The coupled computational model of viscoplasticity and ductile damage, combined with Gruneisen EOS was used for the target plate. Considering the comparatively small deformation that happened in the projectile, an elastic material model was used for the projectile material. All the simulation results were agreed with experiments with acceptable accuracy in terms of ballistic limit velocity. Besides, the numerical results of coupling the SPH-FEM method demonstrated higher spatial accuracy and efficiency than that of SPH only and LS-DYNA. What is worthy to notice that the plastic deformation of the projectile may become severe with higher impact velocity, and this absorbs a lot of the initial kinetic energy. More suitable constitutive models should be chosen for the projectile material with a higher velocity impact, as proposed by Ref. [136].

The benefits of the coupled FE-SPH method applied to impact problems are obviously recognized. Numbers of simulations have been implemented in this way such as [131,137–139]. A hybrid method composed of FE analysis and SPH is used to analyze the perforation of steel material and aluminum plates with varying thickness by different projectiles in Ref. [131]. However, the authors claimed that at a lower range of impact velocities, failure behavior in a thin target was not observed correctly mainly due to the tensile instability problem inherent in the SPH method. FE solutions are in better agreement and may be adopted for this range of impact velocities. Zhang and co-workers applied a FEM-SPH-FEM technique in LS-DYNA combined with fragment identification and statistics methods to investigate the debris cloud in HVI [138]. The case of  $d = 9.52$  mm sphere impact plate with 2.2 mm thickness at 6640 m/s was simulated in this study. The quantity, the size, the mass, and the velocity of a specific fragment were computed and investigated with these statistics on the binary graph, obtaining good

simulation results. A coupled SPH-FE model is also used to simulate a metal-jet penetration into a double hull made of different materials – steel and SPS (Sandwich Plate System) in Ref. [139]. The shaped charge was modeled with SPH and the double-hull structure was modeled with FEM; A penalty method was used to treat the interaction between metal-jet particles and target elements during the entire process. The simulation results were compared with experiments and analyzed to acquire a better understanding of the process of a metal-jet penetration into a double-hull structure. More applications of coupled FE-SPH simulations for HVI problems can be found in the Table 3.

## 6. Conclusion

The SPH method has been developed and applied in many different fields including high-velocity impact in the past forty years. The property of particle discretizations makes it naturally suitable for modeling the structures involving large deformations. Although SPH method is known to involve some numerical drawbacks like numerical instabilities, boundary inaccuracy, time-consuming, as well as interface contact, particularly in solid impact problems, a state of the art in this paper witnessed the great success of the SPH method applied to diverse impact problems, mainly showing as:

- As far, different versions of SPH formulations have been developed to improve the comprehensive performance of SPH simulations, like CSPM, Godunov SPH, total Lagrangian SPH, and pseudo-springs SPH, etc. Besides, most of them have been applied to impact problems.
- The SPH formulation involves great compatibility with other different algorithms and then is developed to some coupled numerical methods like Gamma-SPH, FE-SPH,  $\gamma$ -SPH-ALE, etc.
- The most of fragmentation and debris clouds phenomena in HVIs are predicted well by the SPH method thanks to its natural particle property.
- The application of the SPH method has been extended to a diversity of HVI problems, not limited to metallic projectile-target systems. It comes from the developments of constitutive laws for different materials, and also the good compatibility of SPH schemes.

The target of this paper is to summarize the work about SPH modeling ballistic perforation impact on thin structures. The most challenging task for this review is that the target materials in impacts at present include a large variety of materials such as various composite laminates, brittle materials like ceramics, advanced high-strength cementitious materials, as well as multilayered structures consisting of completely different materials. Indeed, the SPH method has also been extended to simulate the ballistic response of soft tissue materials in recent years like [140,141], particularly, to the bird-strick problem involving the SPH modeling of birds body [142–144], which is not involved in this review. This trend can be foretold with the high

**Table 3**

The table lists the SPH simulations on projectile-target system.

Model & techniques	Impact condition	Projectile-Target system			Physical problem
		projectile	Target	behavior law	
3D standard SPH [54]	<ul style="list-style-type: none"> <li>• normal impact</li> <li>• <math>v_0 = 5.55</math> km/s</li> </ul>	copper disk	<ul style="list-style-type: none"> <li>• Al bumber plate</li> <li>• 2.87 mm thick</li> </ul>	<ul style="list-style-type: none"> <li>• elastic-perfectly-plastic law</li> <li>• Mie-Gruneisen</li> </ul>	size of debris clouds
standard SPH in EPIC code [81]	<ul style="list-style-type: none"> <li>• normal impact</li> <li>• <math>v_0 = 2.0\text{--}5.0</math> km/s</li> </ul>	copper rod	<ul style="list-style-type: none"> <li>• steel plate</li> <li>• 2.6/12.7 cm thick</li> </ul>	<ul style="list-style-type: none"> <li>• Johnson-Cook (1983)</li> <li>• Mie-Gruneisen</li> </ul>	debris cloud, penetration craters, spall cases
SPHC code [71]	<ul style="list-style-type: none"> <li>• normal impact</li> <li>• hull impact</li> <li>• oblique impact</li> <li>• 6.0–10 km/s</li> </ul>	Al sphere/disk	<ul style="list-style-type: none"> <li>• Al plate</li> <li>• mm-scale</li> </ul>	<ul style="list-style-type: none"> <li>• elastic-perfectly-plastic law</li> <li>• Johnson-Cook strength model</li> <li>• Mie-Gruneisen</li> </ul>	debris fragments secondary impacts
SPH, MESA, EPIC, CALE codes [80]	<ul style="list-style-type: none"> <li>• normal impact</li> <li>• 6.0–24.5 km/s</li> </ul>	copper sphere	<ul style="list-style-type: none"> <li>• copper plate</li> <li>• 3.0/4.0 cm</li> </ul>	<ul style="list-style-type: none"> <li>• elastic-perfectly-plastic law</li> <li>• Johnson-Cook strength model</li> <li>• Mie-Gruneisen</li> </ul>	crater volume effects of yield strength
Coupled FE-SPH [132]	<ul style="list-style-type: none"> <li>• normal impact</li> <li>• 0.3–3 km/s</li> </ul>	tungsten rod, rigid	<ul style="list-style-type: none"> <li>• Al</li> <li>• Steel</li> </ul>	<ul style="list-style-type: none"> <li>• Johnson-Cook model</li> </ul>	coupled algorithm, the SPH generation algorithm
SPH code [86]	<ul style="list-style-type: none"> <li>• normal impact</li> <li>• 5–7 km/s</li> </ul>	Al sphere	<ul style="list-style-type: none"> <li>• thin plates</li> <li>• different materials</li> </ul>	<ul style="list-style-type: none"> <li>• Johnson-Cook strength model</li> <li>• Tillotson equation</li> </ul>	debris clouds diameters of the craters
SPH code in AUTODYN-2D [82]	<ul style="list-style-type: none"> <li>• normal impact</li> <li>• 6–8 km/s</li> </ul>	Al sphere	<ul style="list-style-type: none"> <li>• thin whipple shield plates</li> <li>• Al</li> <li>• thin Al plates</li> <li>• a triple shield</li> <li>• a 'stuffed' Whipple shield</li> </ul>	<ul style="list-style-type: none"> <li>• Steinberg-Guinan strength model</li> <li>• Mie-Gruneisen</li> <li>• Johnson-Cook yield model</li> <li>• Sesame eos</li> <li>• Polynomial eos</li> </ul>	debris cloud velocity and shape
SPH code in PAM-SHOCK [87]	<ul style="list-style-type: none"> <li>• normal impact</li> <li>• oblique impact</li> <li>• 6–10 km/s</li> </ul>	Al sphere			debris cloud damage to backwall of shield shapes of craters ejecta trajectories
3D SPH code [55]	<ul style="list-style-type: none"> <li>• normal impact</li> <li>• 0.6–2 km/s</li> </ul>	steel cube, deformed	<ul style="list-style-type: none"> <li>• fiber composite</li> <li>• eight-layer laminate</li> <li>• 0.09648 cm</li> </ul>	<ul style="list-style-type: none"> <li>• anisotropic elastic plasticity</li> <li>• Mie-Gruneisen Eos</li> <li>• failure criterion</li> <li>• Johnson-Cook model</li> </ul>	debris clouds and crater and spall
SPH in PAM-SHOCK 3D and AUTODYN 2D hydrocodes [85]	<ul style="list-style-type: none"> <li>• normal impact</li> <li>• 7 km/s</li> </ul>	Al sphere	<ul style="list-style-type: none"> <li>• thin Al plates</li> <li>• triple wall system</li> </ul>	<ul style="list-style-type: none"> <li>• Steinberg-Guinan</li> <li>• Sesame, Shock, Tillotson</li> </ul>	SPH limitations to debris shielding system
2D-SPH code [121]	<ul style="list-style-type: none"> <li>• normal impact</li> <li>• 820–840 m/s</li> </ul>	Lead/steel rod, deformed	<ul style="list-style-type: none"> <li>• steel plate</li> <li>• 6 mm</li> </ul>	<ul style="list-style-type: none"> <li>• elasto-plastic model</li> </ul>	contact algorithm, numerical fractures
3D-SPH code [122]	<ul style="list-style-type: none"> <li>• normal impact</li> <li>• oblique impact</li> <li>• 2000 m/s</li> </ul>	steel cube, deformed	<ul style="list-style-type: none"> <li>• steel plate</li> <li>• 3 mm</li> </ul>	<ul style="list-style-type: none"> <li>• elasto-perfectly-plastic model</li> </ul>	contact algorithm, numerical fractures
Improved SPH (new particle generation and merger techniques) [56]	<ul style="list-style-type: none"> <li>• normal impact</li> <li>• oblique impact</li> <li>• 4.0 km/s</li> </ul>	aluminum sphere, deformed	<ul style="list-style-type: none"> <li>• Gr/Ep laminate</li> <li>• 1–8 layers</li> <li>• 1 mm</li> </ul>	<ul style="list-style-type: none"> <li>• Elastic-plastic of single layer</li> </ul>	damage and debris clouds
Coupled FE-SPH [135]	<ul style="list-style-type: none"> <li>• oblique impact</li> <li>• 400 m/s</li> </ul>	steel rod with ogive-nose, rigid	<ul style="list-style-type: none"> <li>• Al plate</li> <li>• 2.63 cm</li> </ul>	<ul style="list-style-type: none"> <li>• elastic perfectly plastic model</li> <li>• Gruneisen EOS</li> </ul>	the contact potential algorithm
FE-SPH-FE in LS-DYNA [138]	<ul style="list-style-type: none"> <li>• normal impact</li> <li>• 6.64 m/s</li> </ul>	Al, deformed	<ul style="list-style-type: none"> <li>• Al plates</li> <li>• 2 mm</li> </ul>	<ul style="list-style-type: none"> <li>• Johnson-Cook model with EOS</li> </ul>	fragment identification and statistics method, debris clouds
2D SPH [145]	<ul style="list-style-type: none"> <li>• normal impact</li> <li>• 0.3–3.1 km/s</li> </ul>	Al/Lead/Steel spheres	<ul style="list-style-type: none"> <li>• 2 mm plates</li> <li>• Al/Lead/Steel</li> </ul>	<ul style="list-style-type: none"> <li>• elastic-perfectly plastic law</li> </ul>	the effects of impact velocity and target thickness on penetration depth and crater size
SPH in LS-Dyna [88]	<ul style="list-style-type: none"> <li>• normal impact</li> <li>• 7 km/s</li> </ul>	54R B32 API hardened steel core ammunition	<ul style="list-style-type: none"> <li>• 500 HB armor steel</li> <li>• 9–20 mm</li> </ul>	<ul style="list-style-type: none"> <li>• Johnson-Cook model</li> <li>• Mie-Gruneisen</li> </ul>	ballistic limit, spall and fragmentation
Combined Particle-Element Method (CPEM) [130]	<ul style="list-style-type: none"> <li>• oblique impact</li> <li>• 2 km/s</li> </ul>	Steel, deformed	<ul style="list-style-type: none"> <li>• Steel plate</li> <li>• mm-scale</li> </ul>		element-particle convert and contact algorithms
3D SPH code [57]	<ul style="list-style-type: none"> <li>• normal impact</li> <li>• 200–1200 m/s</li> </ul>	steel ball, deformed	<ul style="list-style-type: none"> <li>• CRFP laminate</li> <li>• 1.6 mm</li> </ul>	<ul style="list-style-type: none"> <li>• Elastic-plastic of single layer</li> <li>• Chang-Chang critera</li> </ul>	damage pattern, fiber breaks, cracks

(continued on next page)

Table 3 (continued)

Model & techniques	Impact condition	Projectile-Target system			Physical problem
		projectile	Target	behavior law	
SPH in LS-Dyna and Eulerian-based hydrocode CTH [89], [90], SPH in Abaqus [58]	<ul style="list-style-type: none"> <li>normal impact</li> <li>4.5–6 km/s</li> </ul>	Lexan cylinder	<ul style="list-style-type: none"> <li>A36 steel target plates</li> <li>12.7 mm</li> </ul>	<ul style="list-style-type: none"> <li>Johnson-Cook model</li> <li>Mie-Gruneisen</li> </ul>	Crater diameter, Penetration Bulge, numerical settings
SPH in LS-Dyna Eulerian-based hydrocode CTH [91]	<ul style="list-style-type: none"> <li>normal impact</li> <li>1067–1097 m/s</li> <li>normal impact</li> <li>80–405.7 m/s</li> </ul>	MIL-P-46593A Standard fragment simulating projectile (FSP), 4340-H Steel, rigid and deformed	<ul style="list-style-type: none"> <li>single plate</li> <li>stacked double-plate</li> <li>cementitious</li> <li>11.9 mm</li> <li>monolithic and layered plates</li> <li>Weldox 460 E steel</li> <li>2–12 mm</li> <li>monolithic and layered plates</li> <li>Weldox 460 E steel</li> <li>8–10 mm</li> <li>monolithic and layered plates</li> <li>Weldox 460 E steel</li> <li>2024-T351 Al alloy</li> <li>6–16 mm</li> <li>ceramic plates</li> <li>ceramic-metal composite plates</li> <li>9–30 mm</li> <li>Al plates</li> <li>mm-scale</li> </ul>	<ul style="list-style-type: none"> <li>Advanced Fundamental Concrete (AFC) model</li> <li>user-defined material model</li> <li>modified Johnson-Cook model</li> <li>viscoplasticity and damage</li> <li>Johnson-Cook plasticity</li> <li>perfectly plasticity</li> </ul>	ballistic limit, spalling, crack propagation
pseudo-spring SPH [38]	<ul style="list-style-type: none"> <li>normal impact</li> <li>100–300 m/s</li> </ul>	Arne tool steel cone			effects of target thickness and number of layers for ballistic resistance
pseudo-spring SPH [39]	<ul style="list-style-type: none"> <li>normal impact</li> <li>70–500 m/s</li> </ul>	Weldox 460 E steel cylinder			crack propagation
pseudo-spring SPH [62]	<ul style="list-style-type: none"> <li>normal impact</li> <li>700–2259 m/s</li> </ul>	Weldox 460 E steel cylinder		<ul style="list-style-type: none"> <li>Johnson-Cook model</li> <li>six damage models</li> </ul>	perforations
$\gamma$ -SPH-ALE [101]	<ul style="list-style-type: none"> <li>normal impact</li> <li>oblique impact</li> <li>4–7 km/s</li> </ul>	cylinders with nose shapes (blunt, hemi-spherical and conical)		<ul style="list-style-type: none"> <li>Johnson-Holmquist I and II</li> <li>Johnson-Holmquist-Bassel</li> <li>Elastic perfectly Plastic</li> <li>Mie-Grüneisen</li> </ul>	spall plane, cracks, numerical parameters sensitivity
GAMMA-SPH [43]	<ul style="list-style-type: none"> <li>normal impact</li> <li>oblique impact</li> <li>4–7 km/s</li> </ul>	Al sphere, Lexan cylinder	<ul style="list-style-type: none"> <li>Al plates with 0.8–4 mm</li> <li>steel plates with 12.7 mm</li> </ul>	<ul style="list-style-type: none"> <li>linear elastic-plastic model</li> <li>Mie-Grüneisen</li> </ul>	debris clouds and crater and spall
SPH code [116]	<ul style="list-style-type: none"> <li>normal impact</li> <li>3.1 km/s</li> </ul>	Al/Steel spheres, deformed	<ul style="list-style-type: none"> <li>Al/Steel plate</li> <li>0.2 cm</li> </ul>	<ul style="list-style-type: none"> <li>Elastic-perfectly plastic model</li> <li>Steinberg-Guinan model</li> <li>Mie-Grüneisen equation</li> <li>HOM equation</li> <li>Johnson Holmquist model</li> <li>pressure cut-off criteria</li> </ul>	shapes of debris clouds, effects of types of artificial viscosities
SPH in LS-DYNA [59]	<ul style="list-style-type: none"> <li>normal impact</li> <li>1–4 km/s</li> </ul>	steel sphere, deformed	<ul style="list-style-type: none"> <li>fused silica plates</li> <li>disposable debris shields (DDS)</li> <li>2–10 mm</li> </ul>		debris cloud, perforation hole and spallation zones
SPH in LS-DYNA [137]	<ul style="list-style-type: none"> <li>normal impact</li> <li>70–1050 m/s</li> </ul>	Caliber/steel/Al, deformed	<ul style="list-style-type: none"> <li>Al/steel/brass plates</li> <li>3–12 mm</li> </ul>	<ul style="list-style-type: none"> <li>Johnson-Cook model with EOS</li> </ul>	residual velocities, ballistic limit, perforation
3D-SPH code [126]	<ul style="list-style-type: none"> <li>normal impact</li> <li>200 m/s</li> </ul>	steel sphere, deformed	<ul style="list-style-type: none"> <li>steel plate</li> <li>1 mm</li> </ul>	<ul style="list-style-type: none"> <li>elasto-plastic model</li> <li>Mie-Grüneisen</li> </ul>	contact algorithm, numerical fractures
SPH and MPM [19]	<ul style="list-style-type: none"> <li>normal impact</li> <li>6150 m/s</li> </ul>	Al sphere, deformed	<ul style="list-style-type: none"> <li>Al plate</li> <li>0.8 mm</li> </ul>	<ul style="list-style-type: none"> <li>Elastic-plastic model</li> <li>Mie-Grüneisen equation</li> </ul>	shapes of debris clouds
SPH in LS-DYNA [131]	<ul style="list-style-type: none"> <li>normal impact</li> <li>10–400 m/s</li> </ul>	steel rod with various noses, rigid	<ul style="list-style-type: none"> <li>steel/Al plates</li> <li>6–30 mm</li> </ul>	<ul style="list-style-type: none"> <li>Johnson-Cook model with EOS</li> </ul>	residual and ballistic limit velocities, perforation
SPH-FEM coupled [136]	<ul style="list-style-type: none"> <li>normal impact</li> <li>180–300 m/s</li> </ul>	steel cylinder, rigid	<ul style="list-style-type: none"> <li>Weldox 460 E steel</li> <li>12 mm</li> </ul>	<ul style="list-style-type: none"> <li>Viscoplasticity and ductile damage model</li> <li>Mie-Grüneisen equation</li> </ul>	coupling algorithm, ballistic limit velocity.
modified SPH [146]	<ul style="list-style-type: none"> <li>normal impact</li> <li>6.18/6.7 km/s</li> </ul>	Al sphere, deformed	<ul style="list-style-type: none"> <li>Al plate</li> <li>mm-scale</li> </ul>	<ul style="list-style-type: none"> <li>not introduced</li> </ul>	boundary deficiencies, shapes of formed craters and apertures.
FE-SPH code [72]	<ul style="list-style-type: none"> <li>normal impact</li> <li>200–400 m/s</li> </ul>	steel cylinder with blunt, conical, ogival noses, rigid	<ul style="list-style-type: none"> <li>Steel/Al plates</li> <li>6–20 mm</li> </ul>	<ul style="list-style-type: none"> <li>modified Johnson-Cook (MJC) model</li> </ul>	residual and ballistic limit velocities
SPH with artificial stress and Godunov scheme [119]	<ul style="list-style-type: none"> <li>normal impact</li> <li>3.1 km/s</li> </ul>	Al/Steel spheres, deformed	<ul style="list-style-type: none"> <li>Al/Steel plate</li> <li>0.2 cm</li> </ul>	<ul style="list-style-type: none"> <li>Elastic-perfectly plastic model</li> <li>Steinberg-Guinan model</li> <li>Mie-Grüneisen equation</li> <li>HOM equation</li> <li>Johnson-Cook model</li> <li>Jones-Wilkins-Lee (JWL)</li> </ul>	tensile instability, shapes of debris clouds
FE-SPH code [139]	<ul style="list-style-type: none"> <li>normal impact</li> <li>200–400 m/s</li> </ul>	Al sphere, metal jet	<ul style="list-style-type: none"> <li>double hull structure</li> </ul>		the penetration process and the damage response

(continued on next page)

**Table 3 (continued)**

Model & techniques	Impact condition	Projectile-Target system		Physical problem
		projectile	Target	
SPH in LY-DYNA [147]	<ul style="list-style-type: none"> <li>• normal impact</li> <li>• oblique impact</li> <li>• 5–6 km/s</li> </ul>	polycarbonate 2 mm-cube, deformed	<ul style="list-style-type: none"> <li>• copper/steel/SPS (Sandwich Plate System)</li> <li>• mm-scale</li> <li>• Al plates</li> <li>• double-plate structure</li> <li>• 0.5–1.5 mm</li> </ul>	<ul style="list-style-type: none"> <li>• Mie-Grüneisen</li> <li>• Johnson-Cook model</li> <li>• Mie-Grüneisen</li> </ul> <p>debris cloud, secondary impact for witness plates, craters</p>
SPH-FE in ABAQUS/ Explicit [134].	<ul style="list-style-type: none"> <li>• normal impact</li> <li>• 5–200 m/s</li> </ul>	rods with noses (conical, hemispherical, blunt), rigid	<ul style="list-style-type: none"> <li>• Al plates</li> <li>• 4 mm</li> </ul>	<ul style="list-style-type: none"> <li>• Johnson-Cook model</li> <li>• Mie-Grüneisen</li> </ul> <p>residual velocities, failure mechanisms and energy absorption</p>
3D SPH-GPU code [125]	<ul style="list-style-type: none"> <li>• normal impact</li> <li>• 130–400 m/s</li> </ul>	steel cylinder, rigid	<ul style="list-style-type: none"> <li>• Weldox 460 E steel</li> <li>• 8–12 mm</li> </ul>	<ul style="list-style-type: none"> <li>• Johnson-Cook model</li> <li>• Mie-Grüneisen equation</li> </ul> <p>GPU technique, residual velocities.</p>
SPH in LS-DYNA combined machine learning techniques [94]	<ul style="list-style-type: none"> <li>• normal impact</li> <li>• 2.15 or 6.64 km/s</li> </ul>	Al, Steel, cylinder, sphere, deformed	<ul style="list-style-type: none"> <li>• Al plates</li> <li>• mm-scale</li> </ul>	<ul style="list-style-type: none"> <li>• Johnson-Cook model</li> <li>• Mie-Grüneisen</li> </ul> <p>residual velocity, hole diameter, and spalling diameter, debris clouds</p>
SPH in LS-DYNA [76]	<ul style="list-style-type: none"> <li>• normal impact</li> <li>• 1.93–4.96 km/s</li> </ul>	Al sphere, deformed	<ul style="list-style-type: none"> <li>• carbon fiber reinforced polymer composites (CFRP)</li> <li>• 2.3 mm</li> <li>• Al plates</li> <li>• 0.4 cm</li> </ul>	<ul style="list-style-type: none"> <li>• MAT_59 material model in LS-DYNA</li> </ul> <p>crater diameters, the secondary debris cloud, ballistic limit</p>
Improved SPH with KGC [98]	<ul style="list-style-type: none"> <li>• normal impact</li> <li>• 4–7 km/s</li> </ul>	Al sphere and cylinder	<ul style="list-style-type: none"> <li>• Al plates</li> <li>• 0.4 cm</li> </ul>	evolution of the debris cloud and particle distribution.
Improved SPH with KGC [100]	<ul style="list-style-type: none"> <li>• normal impact</li> <li>• 2–11 km/s</li> </ul>	Al sphere	<ul style="list-style-type: none"> <li>• Al plates</li> <li>• 0.4 cm</li> </ul>	the sizes of the craters
Corrective SPH (DFPM) [104]	<ul style="list-style-type: none"> <li>• normal impact</li> <li>• oblique impact</li> <li>• 2–12 km/s</li> </ul>	Cu, Al, deformed	<ul style="list-style-type: none"> <li>• Al plates</li> <li>• 2–4 mm</li> </ul>	the craters size and debris clouds
SPH in LS-DYNA (contact model: PCM and PAM) [60]	<ul style="list-style-type: none"> <li>• normal impact</li> <li>• 903 m/s</li> </ul>	alloy, deformed	<ul style="list-style-type: none"> <li>• AL2O3 ceramic</li> <li>• 12.7 mm</li> </ul>	<ul style="list-style-type: none"> <li>• JHI-2 model</li> </ul> <p>contact algorithm, fragmentation, residual velocity</p>

requirements of the modern industry. Therefore, to investigate the HVIs by SPH method in further work still should pay many effects like,

- Tensile instability is still an important factor to affect the simulation accuracy. Although lots of improvements have been developed, the performance of them still depends on the impact conditions like low or high impact velocity, the types of materials. Total Lagrangian SPH seems a comparatively stable scheme, but it needs more applications to different HVI systems to validate its performance.
- The behavior of crack propagation as one of the most important damages during impacts, very depends on the types of materials and target structures, particularly for some multilayered structures or laminated composites. There is no much simulation in this situation. To the best of the authors' knowledge, Pseudo-spring SPH seems the most promising scheme for this.
- The investigations to fragmentation and debris clouds during HVIs are still on the qualitative analysis. The quantitative analysis is necessary, but it is a challenging work for SPH application.
- The other important further work is about developing the material constitutive law compatible with SPH formulas. Especially, the advanced and complex materials are incorporated into the impact systems.

To sum up, although there are still drawbacks that should be improved and further researched, undoubtedly, the SPH method has become a very promising and practical tool for the understanding of high-velocity impact problems.

## Declaration of competing interest

The authors declare that they have no known competing financial interests or personal relationships that could have appeared to influence the work reported in this paper.

## Acknowledgments

Authors thank Chinese Scholarship Council for its financial support.

## References

- [1] A. Bogdan, A. Marszalek, K. Majchrzycka, A. Brochocka, A. Luczak, M. Zwolinska, Aspects of applying ergonomic tests in the evaluation of ballistic body armours using the example of ballistic vests, *J. Textil. Sci. Eng.* 2 (7) (2012) 1–5.
- [2] N.V. David, X.-L. Gao, J.Q. Zheng, Ballistic resistant body armor: contemporary and prospective materials and related protection mechanisms, *Appl. Mech. Rev.* 62 (5) (2009).
- [3] A. Jonas, Zukas. *Introduction to Hydrocodes*, Elsevier, 2004.
- [4] Predrag M. Elek, Slobodan S. Jaramaz, Dejan M. Micković, Nenad M. Miloradović, Experimental and numerical investigation of perforation of thin steel plates by deformable steel penetrators, *Thin-Walled Struct.* 102 (may 2016) 58–67.
- [5] G. Wijk, A. Collin, R. Amiree, Sphere penetration into gelatine and board, in: *The 19th International Symposium of Ballistics*, 2001, pp. 1019–1027.
- [6] L. Liu, Y. Fan, W. Li, H. Liu, Cavity dynamics and drag force of high-speed penetration of rigid spheres into 10wt% gelatin, *Int. J. Impact Eng.* 50 (2012) 68–75.
- [7] M. Philip, Cunniff. A semiempirical model for the ballistic impact performance of textile-based personnel armor, *Textil. Res. J.* 66 (1) (jan 1996) 45–58.
- [8] G. Ben-Dor, A. Dubinsky, T. Elperin, Estimation of perforation thickness for concrete shield against high-speed impact, *Nucl. Eng. Des.* 240 (5) (2010) 1022–1027.

- [9] T. Borvik, K. Vestli, M. Langseth, Determination of projectile path during ballistic penetration by use of a high-speed digital camera, in: Association of High-Speed Photography Conference, 1997.
- [10] T. Borvik, K. Holen, M. Langseth, K.A. Malo, An experimental set-up used in ballistic penetration, *WIT Trans. Built Environ.* 32 (Jan 1998).
- [11] A. Arias, J.A. Rodríguez-Martínez, A. Rusinek, Numerical simulations of impact behaviour of thin steel plates subjected to cylindrical, conical and hemispherical non-deformable projectiles, *Eng. Fract. Mech.* 75 (6) (apr 2008) 1635–1656.
- [12] Andrea Manes, Davide Lumassi, Lorenzo Giudici, Marco Giglio, An experimental-numerical investigation on aluminium tubes subjected to ballistic impact with soft core 7.62 ball projectiles, *Thin-Walled Struct.* 73 (2013) 68–80.
- [13] Milan Žmindiák, Zoran Pelagić, Pastorek Peter, Martin Močilan, Vybosť Šok Martin, Finite element modelling of high velocity impact on plate structures, *Procedia Eng.* 136 (2016) 162–168.
- [14] R.A. Gingold, J.J. Monaghan, Smoothed particle hydrodynamics - theory and application to non-spherical stars, *Mon. Not. Roy. Astron. Soc.* 181 (1977) 375–389.
- [15] L.B. Lucy, A numerical approach to the testing of the fission hypothesis, *Astron. J.* 82 (12) (1977) 1013–1024.
- [16] Sophie Adélaïde Magnier, Frédéric-Victor Donzé, Numerical simulations of impacts using a discrete element method, *Mechanics of Cohesive-frictional Materials*, *Int. J. Exp. Model. Comput. Mater. Struct.* 3 (3) (1998) 257–276.
- [17] Antonio A. Munjiza, *The Combined Finite-Discrete Element Method*, John Wiley & Sons, 2004.
- [18] Ting Ye, Li Yu, A comparative review of smoothed particle hydrodynamics, dissipative particle dynamics and smoothed dissipative particle dynamics, *Int. J. Comput. Methods* 15 (8) (2018) 1–19.
- [19] S. Ma, X. Zhang, X.M. Qiu, Comparison study of MPM and SPH in modeling hypervelocity impact problems, *Int. J. Impact Eng.* 36 (2) (2009) 272–282.
- [20] Matthias Röthlin, Hagen Klippl, Konrad Wegener, Meshless Methods for Large Deformation Elastodynamics, 2018 arXiv preprint arXiv:1807.01117.
- [21] Ted Belytschko, Yury Krongauz, Daniel Organ, Mark Fleming, Petr Krysl, Meshless methods: an overview and recent developments, *Comput. Methods Appl. Mech. Eng.* 139 (1) (1996) 3–47.
- [22] Shaofan Li, Wing Kam Liu, Meshfree and particle methods and their applications, *Appl. Mech. Rev.* 55 (1) (2002) 1–34.
- [23] P.W. Randles, L.D. Libersky, Smoothed particle hydrodynamics: some recent improvements and applications, *Comput. Methods Appl. Mech. Eng.* 139 (1–4) (dec 1996) 375–408.
- [24] Larry D. Libersky, Albert G. Petschek, Theodore C. Carney, Jim R. Hipp, Firooz A. Allahdadi, High strain Lagrangian hydrodynamics, *J. Comput. Phys.* 109 (1) (nov 1993) 67–75.
- [25] Marvin E. Backman, Werner Goldsmith, The mechanics of penetration of projectiles into targets, *Int. J. Eng. Sci.* 16 (1) (1978) 1–99.
- [26] J.W. Swegle, D.L. Hicks, S.W. Attaway, Smoothed particle hydrodynamics stability analysis, *J. Comput. Phys.* 116 (1) (1995) 123–134.
- [27] Joseph J. Monaghan, Robert A. Gingold, Shock simulation by the particle method sph, *J. Comput. Phys.* 52 (2) (1983) 374–389.
- [28] J.J. Monaghan, On the problem of penetration in particle methods, *J. Comput. Phys.* 82 (1) (1989) 1–15.
- [29] Joseph J. Monaghan, Sph without a tensile instability, *J. Comput. Phys.* 159 (2) (2000) 290–311.
- [30] James P. Gray, Joseph J. Monaghan, R.P. Swift, Sph elastic dynamics, *Comput. Methods Appl. Mech. Eng.* 190 (49–50) (2001) 6641–6662.
- [31] J.K. Chen, J.E. Beraun, C.J. Jih, An improvement for tensile instability in smoothed particle hydrodynamics, *Comput. Mech.* 23 (4) (1999) 279–287.
- [32] Keisuke Suguri, Shu-ichiro Inutsuka, An extension of godunov sph: application to negative pressure media, *J. Comput. Phys.* 308 (2016) 171–197.
- [33] Shu-ichiro Inutsuka, Reformulation of Smoothed Particle Hydrodynamics with Riemann Solver, 2002 arXiv preprint astro-ph/0206401.
- [34] Timon Rabczuk, T. Belytschko, S.P. Xiao, Stable particle methods based on lagrangian kernels, *Comput. Methods Appl. Mech. Eng.* 193 (12–14) (2004) 1035–1063.
- [35] Juan R. Reveles, Development of a Total Lagrangian Sph Code for the Simulation of Solids under Dynamic Loading, 2007.
- [36] Georg C. Ganzemüller, An hourglass control algorithm for lagrangian smooth particle hydrodynamics, *Comput. Methods Appl. Mech. Eng.* 286 (2015) 87–106.
- [37] Sukanta Chakraborty, Shaw Amit, A pseudo-spring based fracture model for sph simulation of impact dynamics, *Int. J. Impact Eng.* 58 (2013) 84–95.
- [38] Md Rushdie Ibne Islam, Sukanta Chakraborty, Shaw Amit, Stephen Reid, A computational model for failure of ductile material under impact, *Int. J. Impact Eng.* 108 (2017) 334–347.
- [39] Md Rushdie Ibne Islam, Shaw Amit, Pseudo-spring sph simulations on the perforation of metal targets with different damage models, *Eng. Anal. Bound. Elem.* 111 (2020) 55–77.
- [40] Gary A. Dilts, Moving-least-squares-particle hydrodynamics i. consistency and stability, *Int. J. Numer. Methods Eng.* 44 (8) (1999) 1115–1155.
- [41] Gary A. Dilts, Moving least-squares particle hydrodynamics ii: conservation and boundaries, *Int. J. Numer. Methods Eng.* 48 (10) (2000) 1503–1524.
- [42] Diego Molteni, Andrea Colagrossi, A simple procedure to improve the pressure evaluation in hydrodynamic context using the sph, *Comput. Phys. Commun.* 180 (6) (2009) 861–872.
- [43] Jérôme Limido, Trabia Mohamed, Shawoon Roy, Brendan O'Toole, Richard Jennings, Wayne L. Mindle, Michael Pena, Edward Daykin, Robert Hixson, Melissa Matthes, Modeling of hypervelocity impact experiments using gamma-sph technique, in: ASME 2017 Pressure Vessels and Piping Conference, American Society of Mechanical Engineers Digital Collection, 2017.
- [44] M.B. Liu, G.R. Liu, Smoothed particle hydrodynamics (sph): an overview and recent developments, *Arch. Comput. Methods Eng.* 17 (1) (2010) 25–76.
- [45] Joseph J. Monaghan, Smoothed particle hydrodynamics and its diverse applications, *Annu. Rev. Fluid Mech.* 44 (2012) 323–346.
- [46] Gordon R. Johnson, Artificial viscosity effects for sph impact computations, *Int. J. Impact Eng.* 18 (5) (1996) 477–488.
- [47] Gordon R. Johnson, Stephen R. Beissel, Normalized smoothing functions for sph impact computations, *Int. J. Numer. Methods Eng.* 39 (16) (1996) 2725–2741.
- [48] J.K. Chen, J.E. Beraun, T.C. Carney, A corrective smoothed particle method for boundary value problems in heat conduction, *Int. J. Numer. Methods Eng.* 46 (2) (1999) 231–252.
- [49] J.K. Chen, J.E. Beraun, A generalized smoothed particle hydrodynamics method for nonlinear dynamic problems, *Comput. Methods Appl. Mech. Eng.* 190 (1–2) (2000) 225–239.
- [50] R.C. Batra, G.M. Zhang, Analysis of adiabatic shear bands in elasto-thermo-viscoplastic materials by modified smoothed-particle hydrodynamics (msph) method, *J. Comput. Phys.* 201 (1) (2004) 172–190.
- [51] Rade Vignjević, Juan R. Reveles, James Campbell, Sph in a Total Lagrangian Formalism, vol. 4, CMC-Tech Science Press-, 2006, p. 181, 3.
- [52] M.B. Liu, Gui-Rong Liu, Restoring particle consistency in smoothed particle hydrodynamics, *Appl. Numer. Math.* 56 (1) (2006) 19–36.
- [53] Larry D. Libersky, A.G. Petschek, Smooth particle hydrodynamics with strength of materials, in: *Advances in the Free-Lagrange Method Including Contributions on Adaptive Gridding and the Smooth Particle Hydrodynamics Method*, Springer Berlin Heidelberg, Berlin, Heidelberg, 1991, pp. 248–257.
- [54] A.G. Petschek, L.D. Libersky, Cylindrical smoothed particle hydrodynamics, *J. Comput. Phys.* 109 (1) (nov 1993) 76–83.
- [55] J.K. Chen, F.A. Allahdadi, T.C. Carney, High-velocity impact of graphite/epoxy composite laminates, *Compos. Sci. Technol.* 57 (9–10) (1997) 1369–1379.
- [56] K. Shintate, H. Sekine, Numerical simulation of hypervelocity impacts of a projectile on laminated composite plate targets by means of improved sph method, *Compos. Appl. Sci. Manuf.* 35 (6) (2004) 683–692.
- [57] S. Yashiro, K. Ogi, A. Yoshimura, Y. Sakaida, Characterization of high-velocity impact damage in CFRP laminates: Part II – prediction by smoothed particle hydrodynamics, *Compos. Appl. Sci. Manuf.* 56 (2014) 308–318.
- [58] William F Heard Nikolas A Nordendale, A Sherburn Jesse, Prodyot K. Basu, A comparison of finite element analysis to smooth particle hydrodynamics for application to projectile impact on cementitious material, *Comput. Part. Mech.* 3 (1) (2016) 53–68.
- [59] Y. Michel, J.-M.J. Chevalier, C. Durin, C. Espinosa, F. Malaise, J.-J.J. Barraud, Hypervelocity impacts on thin brittle targets: experimental data and SPH simulations, *Int. J. Impact Eng.* 33 (1–12) (dec 2006) 441—451.
- [60] Yihua Xiao, Hecheng Wu, Xuecheng Ping, On the simulation of fragmentation during the process of ceramic tile impacted by blunt projectile with sph method, *Comput. Model. Eng. Sci.* 122 (3) (2020) 923–954.
- [61] Yihui Zhu, G.R. Liu, Yaoke Wen, Cheng Xu, Weilong Niu, Guangyu Wang, Back-spalling process of an al2o3 ceramic plate subjected to an impact of steel ball, *Int. J. Impact Eng.* 122 (2018) 451–471.
- [62] Md Rushdie Ibne Islam, J.Q. Zheng, Romesh C. Batra, Ballistic performance of ceramic and ceramic-metal composite plates with jh1, jh2 and jhb material models, *Int. J. Impact Eng.* 137 (2020) 103469.
- [63] Riccardo Scazzosi, Marco Giglio, Andrea Manes, Fe coupled to sph numerical model for the simulation of high-velocity impact on ceramic based ballistic shields, *Ceram. Int.* (2020).
- [64] T. Borvik, M. Langseth, O.S. Hopperstad, K.A. Malo, Ballistic penetration of steel plates, *Int. J. Impact Eng.* 22 (9–10) (1999) 855–886.
- [65] Andrea Manes, Davide Lumassi, Lorenzo Giudici, Marco Giglio, An experimental-numerical investigation on aluminium tubes subjected to ballistic impact with soft core 7.62 ball projectiles, *Thin-Walled Struct.* 73 (2013) 68–80.
- [66] Andrew J. Piekutowski, Characteristics of debris clouds produced by hypervelocity impact of aluminum spheres with thin aluminum plates, *Int. J. Impact Eng.* 14 (1–4) (1993) 573–586.
- [67] Joseph J. Monaghan, An introduction to sph, *Comput. Phys. Commun.* 48 (1988) 89–96.
- [68] W. Benz, A.G.W. Cameron, H.J. Melosh, The origin of the moon and the single-impact hypothesis iii, *Icarus* 81 (1) (1989) 113–131.
- [69] Phil M. Campbell, Some New Algorithms for Boundary Value Problems in Smooth Particle Hydrodynamics, Technical report, MISSION RESEARCH CORP ALBUQUERQUE NM, 1989.
- [70] Gordon R. Johnson, William H. Cook, A constitutive model and data for metals subjected to large strains, high strain rates and high temperatures, in: Proceedings of the 7th International Symposium on Ballistics, vol. 21, 1983, pp. 541–547. The Netherlands.
- [71] R.F. Stellingwerf, C.A. Wingate, Impact modeling with smooth particle hydrodynamics, *Int. J. Impact Eng.* 14 (1–4) (jan 1993) 707–718.
- [72] Z.S. Liu, S. Swadhiwupong, M.J. Islam, Perforation of steel and aluminum targets using a modified johnson-cook material model, *Nucl. Eng. Des.* 250 (2012) 108–115.
- [73] Gordon R. Johnson, Tim J. Holmqvist, An improved computational constitutive model for brittle materials, in: AIP Conference Proceedings, vol. 309, American Institute of Physics, 1994, pp. 981–984.
- [74] Dongxi Lv, Yuanming Zhang, Numerical simulation of chipping formation process with smooth particle hydrodynamic (sph) method for diamond drilling ain ceramics, *Int. J. Adv. Manuf. Technol.* 96 (5–8) (2018) 2257–2269.

- [75] D.F. Medina, J.K. Chen, Three-dimensional simulations of impact induced damage in composite structures using the parallelized sph method, *Compos. Appl. Sci. Manuf.* 31 (8) (2000) 853–860.
- [76] E. Giannatos, A. Kotzakios, V. Kostopoulos, G. Campoli, Hypervelocity impact response of cfrp laminates using smoothed particle hydrodynamics method: implementation and validation, *Int. J. Impact Eng.* 123 (2019) 56–69.
- [77] F. Robert, Stellingwerf. Smooth particle hydrodynamics, in: *Advances in the Free-Lagrange Method Including Contributions on Adaptive Gridding and the Smooth Particle Hydrodynamics Method*, Springer Berlin Heidelberg, Berlin, Heidelberg, 1991, pp. 239–247.
- [78] D. Lawrence, Cloutman. An evaluation of smoothed particle hydrodynamics, in: *Advances in the Free-Lagrange Method Including Contributions on Adaptive Gridding and the Smooth Particle Hydrodynamics Method*, Springer Berlin Heidelberg, Berlin, Heidelberg, 1991, pp. 227–238.
- [79] Gordon R. Johnson, Robert A. Stryk, Jack G. Dodd, Dynamic Lagrangian computations for solids, with variable nodal connectivity for severe distortions, *Int. J. Numer. Methods Eng.* 23 (3) (mar 1986) 509–522.
- [80] C.A. Wingate, R.F. Stellingwerf, R.F. Davidson, M.W. Burkett, Models of high velocity impact phenomena, *Int. J. Impact Eng.* 14 (1–4) (1993) 819–830.
- [81] Gordon R. Johnson, Eric H. Petersen, Robert A. Stryk, Incorporation of an SPH Option into the EPIC Code for a Wide Range of High Velocity Impact Computations, jan 1993.
- [82] Colin J. Hayhurst, Richard A. Clegg, Cylindrically symmetric sph simulations of hypervelocity impacts on thin plates, *Int. J. Impact Eng.* 20 (1–5) (1997) 337–348.
- [83] J.W. Swegle, S.W. Attaway, M.W. Heinstein, F.J. Mello, D.L. Hicks, An Analysis of Smoothed Particle Hydrodynamics, Technical report, Sandia National Labs., Albuquerque, NM (United States), 1994.
- [84] Dinshaw S. Balsara, Von neumann stability analysis of smoothed particle hydrodynamicsâ“ suggestions for optimal algorithms, *J. Comput. Phys.* 121 (2) (1995) 357–372.
- [85] Faraud Moreno, Roberto Destefanis, David Palmieri, Mario Marchetti, SPH simulations of debris impacts using two different computer codes, *Int. J. Impact Eng.* 23 (1) (dec 1999) 249–260.
- [86] S. Hiermaier, D. Könke, A.J. Stilp, K. Thoma, Computational simulation of the hypervelocity impact of al-spheres on thin plates of different materials, *Int. J. Impact Eng.* 20 (1–5) (1997) 363–374.
- [87] Paul H.L. Groenboom, Numerical simulation of 2D and 3D hypervelocity impact using the SPH option in PAM-SHOCKâ„¢, *Int. J. Impact Eng.* 20 (1–5) (jan 1997) 309–323.
- [88] Namik Küçük, Bülent Ekici, Ballistic resistance of high hardness armor steels against 7.62 mm armor piercing ammunition, *Mater. Des.* 44 (2013) 35–48.
- [89] Brendan O'Toole, Trabia Mohamed, Robert Hixson, K. Shawoon, S.K. Roy, Michael Pena, Steven Becker, Edward Daykin, Eric Machorro, Richard Jennings, Melissa Matthes, B. O'Toole, Trabia Mohamed, Robert Hixson, K. Shawoon, S. K. Roy, Michael Pena, Steven Becker, Edward Daykin, Eric Machorro, Richard Jennings, Modeling plastic deformation of steel plates in hypervelocity impact experiments, *Procedia Eng.* 103 (jan 2015) 458–465.
- [90] Shawoon K. Roy, Trabia Mohamed, Brendan O'Toole, Robert Hixson, Steven Becker, Michael Pena, Richard Jennings, Deepak Somasundaram, Melissa Matthes, Edward Daykin, et al., Study of hypervelocity projectile impact on thick metal plates, *Shock Vib.* (2016) 2016.
- [91] Yihua Xiao, Huanghuang Dong, Jianmin Zhou, Jungang Wang, Studying normal perforation of monolithic and layered steel targets by conical projectiles with sph simulation and analytical method, *Eng. Anal. Bound. Elem.* 75 (2017) 12–20.
- [92] T. Børvik, O.S. Hopperstad, T. Berstad, M. Langseth, A computational model of viscoplasticity and ductile damage for impact and penetration, *Eur. J. Mech. Solid.* 20 (5) (2001) 685–712.
- [93] Andrew Thurber, Javid Bayandor, On the fluidic response of structures in hypervelocity impacts, *J. Fluide Eng.* 137 (4) (apr 2015), 041101.
- [94] Jae Sakong, Sung-Choong Woo, Tae-Won Kim, Determination of impact fragments from particle analysis via smoothed particle hydrodynamics and k-means clustering, *Int. J. Impact Eng.* 134 (2019) 103387.
- [95] Sukanta Chakraborty, Shaw Amit, Crack propagation in bi-material system via pseudo-spring smoothed particle hydrodynamics, *Int. J. Comput. Methods Eng. Sci. Mech.* 15 (3) (2014) 294–301.
- [96] Sukanta Chakraborty, Shaw Amit, Prognosis for ballistic sensitivity of pre-notch in metallic beam through mesh-less computation reflecting material damage, *Int. J. Solid Struct.* 67 (2015) 192–204.
- [97] Md Rushdie Ibne Islam, Chong Peng, A total lagrangian sph method for modelling damage and failure in solids, *Int. J. Mech. Sci.* 157 (2019) 498–511.
- [98] Z.L. Zhang, M.B. Liu, Smoothed particle hydrodynamics with kernel gradient correction for modeling high velocity impact in two-and three-dimensional spaces, *Eng. Anal. Bound. Elem.* 83 (2017) 141–157.
- [99] J.R. Shao, H.Q. Li, G.R. Liu, M.B. Liu, An improved sph method for modeling liquid sloshing dynamics, *Comput. Struct.* 100 (2012) 18–26.
- [100] Z.L. Zhang, T. Ma, D.L. Feng, M.B. Liu, A new formula for predicting the crater size of a target plate produced by hypervelocity impact, *Int. J. Comput. Methods* 17 (1) (2020) 1844004.
- [101] Collé Anthony, Jérôme Limido, Jean-Paul Vila, An accurate sph scheme for dynamic fragmentation modelling, in: *EPJ Web of Conferences*, vol. 183, EDP Sciences, 2018, 01030.
- [102] J.P. Vila, On particle weighted methods and smooth particle hydrodynamics, *Math. Model Methods Appl. Sci.* 9 (2) (1999) 161–209.
- [103] Gianluca Lavalle, J.-P. Vila, G. Blanchard, Claire Laurent, François Charru, A numerical reduced model for thin liquid films sheared by a gas flow, *J. Comput. Phys.* 301 (2015) 119–140.
- [104] Z.L. Zhang, D.L. Feng, T. Ma, M.B. Liu, Predicting the damage on a target plate produced by hypervelocity impact using a decoupled finite particle method, *Eng. Anal. Bound. Elem.* 98 (2019) 110–125.
- [105] Z.L. Zhang, K. Walayat, C. Huang, J.Z. Chang, M.B. Liu, A finite particle method with particle shifting technique for modeling particulate flows with thermal convection, *Int. J. Heat Mass Tran.* 128 (2019) 1245–1262.
- [106] Shigeki Yashiro, Keiji Ogi, Tsukasa Nakamura, Akinori Yoshimura, Characterization of high-velocity impact damage in cfrp laminates: Part i-experiment, *Compos. Appl. Sci. Manuf.* 48 (2013) 93–100.
- [107] Y. Wen, D.L. Hicks, J.W. Swegle, Stabilizing Sph with Conservative Smoothing, Technical report, Sandia National Labs., Albuquerque, NM (United States), 1994.
- [108] Gordon R. Johnson, Robert A. Stryk, Stephen R. Beissel, Sph for high velocity impact computations, *Comput. Methods Appl. Mech. Eng.* 139 (1–4) (1996) 347–373.
- [109] Hidenori Takeda, Shoken M. Miyama, Minoru Sekiya, Numerical simulation of viscous flow by smoothed particle hydrodynamics, *Prog. Theor. Phys.* 92 (5) (1994) 939–960.
- [110] Larry D. Libersky, Phil W. Randles, Ted C. Carney, David L. Dickinson, Recent improvements in SPH modeling of hypervelocity impact, *Int. J. Impact Eng.* 20 (6–10) (jan 1997) 525–532.
- [111] T. Belytschko, Shaoping Xiao, Stability analysis of particle methods with corrected derivatives, *Comput. Math. Appl.* 43 (3–5) (2002) 329–350.
- [112] Ted Belytschko, Yong Guo, Wing Kam Liu, Shao Ping Xiao, A unified stability analysis of meshless particle methods, *Int. J. Numer. Methods Eng.* 48 (9) (2000) 1359–1400.
- [113] Shaw Amit, Stephen R. Reid, Heuristic acceleration correction algorithm for use in sph computations in impact mechanics, *Comput. Methods Appl. Mech. Eng.* 198 (49–52) (2009) 3962–3974.
- [114] John VonNeumann, Robert D. Richtmyer, A method for the numerical calculation of hydrodynamic shocks, *J. Appl. Phys.* 21 (3) (1950) 232–237.
- [115] Joseph P. Morris, Joseph J. Monaghan, A switch to reduce sph viscosity, *J. Comput. Phys.* 136 (1) (1997) 41–50.
- [116] Vishal Mehra, Shashank Chaturvedi, High velocity impact of metal sphere on thin metallic plates: a comparative smooth particle hydrodynamics study, *J. Comput. Phys.* 212 (1) (feb 2006) 318–337.
- [117] Y.H. Xiao, D.A. Hu, X. Han, G. Yang, S.Y. Long, Simulation of normal perforation of aluminum plates using axisymmetric smoothed particle hydrodynamics with contact algorithm, *Int. J. Comput. Methods* 10 (3) (2013) 1350039.
- [118] A GeZn Petschek, L.D. Libersky, Cylindrical smoothed particle hydrodynamics, *J. Comput. Phys.* 109 (1) (1993) 76–83.
- [119] Vishal Mehra, C.D. Sijoy, Vinayak Mishra, Shashank Chaturvedi, Tensile instability and artificial stresses in impact problems in SPH, *J. Phys. Conf.* 377 (1) (jul 2012), 012102.
- [120] Keisuke Sugiura, Shu-ichiro Inutsuka, An extension of godunov sph ii: application to elastic dynamics, *J. Comput. Phys.* 333 (2017) 78–103.
- [121] Anatoly N. Parshikov, Stanislav A. Medin, Igor I. Loukashenko, Valery A. Milekhin, Improvements in SPH method by means of interparticle contact algorithm and analysis of perforation tests at moderate projectile velocities, *Int. J. Impact Eng.* 24 (8) (sep 2000) 779–796.
- [122] Anatoly N. Parshikov, Stanislav A. Medin, Smoothed particle hydrodynamics using interparticle contact algorithms, *J. Comput. Phys.* 180 (1) (jul 2002) 358–382.
- [123] Alejandro C. Crespo, Jose M. Dominguez, Anxo Barreiro, Moncho Gómez-Gesteira, Benedict D. Rogers, Gpus, a new tool of acceleration in cfd: efficiency and reliability on smoothed particle hydrodynamics methods, *PloS One* 6 (6) (2011), e20685.
- [124] Alexis Héault, Giuseppe Bilotta, Robert A. Dalrymple, Sph on gpu with cuda, *J. Hydraul. Res.* 48 (S1) (2010) 74–79.
- [125] H. Frissane, L. Taddei, N. Lebaal, S. Roth, 3d smooth particle hydrodynamics modeling for high velocity penetrating impact using gpu: application to a blunt projectile penetrating thin steel plates, *Comput. Methods Appl. Mech. Eng.* 357 (2019) 112590.
- [126] Songwon Seo, Oakkey Min, Jaehoon Lee, Application of an improved contact algorithm for penetration analysis in SPH, *Int. J. Impact Eng.* 35 (6) (jun 2008) 578–588.
- [127] S.W. Attaway, M.W. Heinstein, J.W. Swegle, Coupling of smooth particle hydrodynamics with the finite element method, *Nucl. Eng. Des.* 150 (2–3) (1994) 199–205.
- [128] Martin Sauer, Adaptive Kopplung des netzfreien SPH-Verfahrens mit finiten Elementen zur Berechnung von Impaktvorgängen, Universität der Bundeswehr München, 2000.
- [129] J. Campbell, R. Vignjevic, L. Libersky, A contact algorithm for smoothed particle hydrodynamics, *Comput. Methods Appl. Mech. Eng.* 184 (1) (2000) 49–65.
- [130] SR Beissel GR Johnson, C.A. Gerlach, A combined particle-element method for high-velocity impact computations, *Procedia Eng.* 58 (2013) 269–278.
- [131] S. Swaddiwudhipong, M.J. Islam, Z.S. Liu, High velocity penetration/perforation using coupled smooth particle hydrodynamics-finite element method, *Int. J. Prot. Struct.* 1 (4) (2010) 489–506.
- [132] R. Gordon, Johnson. Linking of Lagrangian particle methods to standard finite element methods for high velocity impact computations, *Nucl. Eng. Des.* 150 (2–3) (sep 1994) 265–274.

- [133] Gordon R. Johnson, Robert A. Stryk, Conversion of 3d distorted elements into meshless particles during dynamic deformation, *Int. J. Impact Eng.* 28 (9) (2003) 947–966.
- [134] M. Rodriguez-Millan, D. Garcia-Gonzalez, A. Rusinek, F. Abed, A. Arias, Perforation mechanics of 2024 aluminum protective plates subjected to impact by different nose shapes of projectiles, *Thin-Walled Struct.* 123 (1–10) (2018).
- [135] T. De Vuyst, R. Vignjevic, J.C. Campbell, Coupling between meshless and finite element methods, *Int. J. Impact Eng.* 31 (8) (2005) 1054–1064.
- [136] Zhichun Zhang, Hongfu Qiang, Weiran Gao, Coupling of smoothed particle hydrodynamics and finite element method for impact dynamics simulation, *Eng. Struct.* 33 (1) (2011) 255–264.
- [137] Leonard E. Schwer, Kurt Hacker, Kenneth Poe, Perforation of metal plates: laboratory experiments and numerical simulations, in: Proceedings to the 9th Annual LS DYNA Users Conference, 2006.
- [138] Xiaotian Zhang, Guanghui Jia, Hai Huang, Fragment identification and statistics method of hypervelocity impact sph simulation, *Chin. J. Aeronaut.* 24 (1) (2011) 18–24.
- [139] Z. Zhang, L. Wang, V.V. Silberschmidt, S. Wang, SPH-FEM simulation of shaped-charge jet penetration into double hull: a comparison study for steel and SPS, *Compos. Struct.* 155 (2016) 135–144.
- [140] Monzer Al Khalil, Frissane Hassan, Lorenzo Taddei, Shuangshuang Meng, Nadhir Lebaal, Frederic Demoly, Cynthia Bir, Sébastien Roth, Sph-based method to simulate penetrating impact mechanics into ballistic gelatin: toward an understanding of the perforation of human tissue, *Extreme Mech. Lett.* 29 (2019) 100479.
- [141] H. Frissane, L. Taddei, N. Lebaal, S. Roth, Sph modeling of high velocity impact into ballistic gelatin, development of an axis-symmetrical formulation, *Mech. Adv. Mater. Struct.* 26 (22) (2019) 1881–1888.
- [142] Zhuo Zhang, Li Liang, Dingguo Zhang, Effect of arbitrary yaw/pitch angle in bird strike numerical simulation using sph method, *Aero. Sci. Technol.* 81 (2018) 284–293.
- [143] Yadong Zhou, Youchao Sun, Wenchao Cai, Bird-striking damage of rotating laminates using sph-cdm method, *Aero. Sci. Technol.* 84 (2019) 265–272.
- [144] J. Zhou, J. Liu, X. Zhang, Y. Yan, L. Jiang, I. Mohagheghian, J.P. Dear, M. N. Charalambides, Experimental and numerical investigation of high velocity soft impact loading on aircraft materials, *Aero. Sci. Technol.* 90 (2019) 44–58.
- [145] Hossein Asadi Kalameh, Arash Karamali, Cosmin Anitescu, Timon Rabczuk, High velocity impact of metal sphere on thin metallic plate using smooth particle hydrodynamics (sph) method, *Front. Struct. Civ. Eng.* 6 (2) (2012) 101–110.
- [146] K.A. Alhussan, V.A. Babenko, I.M. Kozlov, A.S. Smetannikov, Development of modified SPH approach for modeling of high-velocity impact, *Int. J. Heat Mass Tran.* 55 (2012) 6340–6348.
- [147] S.A. Ponjaev, R.O. Kurakin, A.I. Sedov, S.V. Bobashev, B.G. Zhukov, A.F. Nechunaev, Hypervelocity impact of mm-size plastic projectile on thin aluminum plate, *Acta Astronaut.* 135 (26–33) (jun 2017).